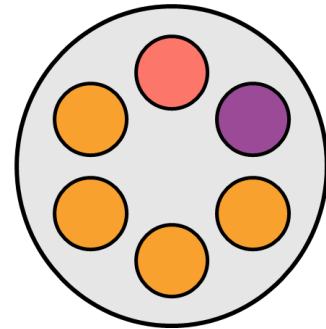


University of Birmingham
School of Engineering

Integrated Design Project 3



FINAL GROUP REPORT MEng Mechanical Engineering

Team Number	3
Group Number	3

Student Names	ID Numbers
Heba Ali	2184931
Zara Iman-Butt	2200848
Mahmood El-Mahalawy	2295059
Waddah Alowadh	2314870
Shelly Tchoutezo	2178158
Sundus Abdirahin	2327470
Hoda Chahini	2109520



Feedback (Compulsory Section)		
Reflecting on the feedback that we have received on previous assessments, the following issues/topics have been identified as areas for improvement:	1	There have been issues with justifying design choices in past reports.
	2	Focus on improving the reliability and durability of the turbine components, addressing potential issues such as fatigue, wear, and environmental degradation over the turbine's lifespan.
	3	Focus on using softwares to back findings
In this assignment, we have attempted to act on previous feedback in the following ways:	1	Finding multiple sources that justify any design choice. For example, the blade design was based on CFD, FEA, calculations and literature.
	2	Conducted detailed analysis and simulations to optimize the blade geometry for improved aerodynamic performance and reduced structural loads, aiming to increase energy capture efficiency.
	3	Multiples softwares use including Granta Edupack, GP100, ANSYS CFX, Fusion360
Feedback on the following aspects of this assignment (i.e. content/style/approach) would be particularly helpful to us:	1	Technical rigor
	2	Clarity and conciseness
	3	Innovation and clarity

Contents

2.1 / PROJECT SUMMARY	20
2.2 / PRODUCT DESIGN SPECIFICATION.....	21
2.3 / PROJECT MANAGEMENT	23
2.4 / RESEARCH.....	27
2.5 / CONCEPT DESIGNS.....	29
2.6 / TECHNICAL EVALUATION OF FINAL DESIGN.....	32
2.7 / MATERIALS SELECTION: MANUFACTURED PARTS	54
2.8 / BILLS OF MATERIALS	65
2.9 / RISK ASSESSMENT	66
2.10 / FINAL DESIGN	68
2.11 / WIDER ENGINEERING IMPLICATIONS.....	70
2.12 / BUSINESS PLAN.....	70
2.13 / ASSEMBLY ROUTE SHEET.....	77
2.14 / MANUFACTURING ROUTE SHEET.....	80
2.15 / OPERATIONS LIST.....	86

2.1 / PROJECT SUMMARY

The following project focuses on manufacturing integral components for a wind turbine located on an offshore energy island near Crete. This report aims to increase Crete's renewable energy output, aligning with its 2050 carbon neutrality goal. The manufacturing will primarily concentrate on turbine blades, which are crucial for enhancing wind turbine efficiency. This effort will be complemented by producing other essential components such as the turbine hub, nose hub and pitch drive.

The primary objectives of the project include optimising the design for maximum energy efficiency and minimising manufacturing costs. This was done by carrying out a thorough technical evaluation which included a detailed calculations section as well as CFD analysis and FEA. The strategic approach promotes sustainability by incorporating sustainable practices in all aspects of the design. A risk assessment and a Failure Mode and Effects Analysis (FMEA) were conducted to highlight the potential hazards and ensure the safety and reliability of the design. The business plan outlines the production strategy and timelines, emphasising cost-effective methods without compromising product quality or efficiency.

The diverse team directing this initiative brings a variety of expertise, from design and calculations to advanced modelling techniques. Such capabilities have allowed for the development of optimal blade designs and efficient manufacturing processes, thus setting new standards in the industry. The goal is not only to support Crete's energy goals but also to establish a model for renewable energy development that could be replicated in other regions.

2.2 / PRODUCT DESIGN SPECIFICATION

The product design specification is outlined below in Table 1.

Table 1: Product Design Specification (PDS)

Aspect	Objective	Criteria
1. Scope	1.1 Optimum design of wind turbine	Twisted and tapered blade design.
	1.2 Quantity	Manufacture components for 26 wind turbines .
2. Design requirements	2.1 Increase structural integrity	Ensure blade max resultant force (F_r) flapwise and edgewise does not exceed 740 kN and 975 kN respectively.
		Ensure max shear force and bending stress for shaft does not exceed 0.4 kN and 0.04 kNm respectively.
		Evaluate fatigue life of material at 10^7 cycles .
		Ensure lift to drag ratio (L/D) lies close to 80 for airfoil tip and 40 for airfoil root.
		Determine optimum angle of attack to be 6.5° .
	2.2 Design with focus on manufacturability	Design components with accessible geometries for manufacturing methods.
Standardise dimensions and tolerances.		
3. Performance	3.1 Ensure optimal turbine operation	Ensure wind turbines achieve a lifespan of 25 years or more .
		Maintain blade speed of 9.5 rpm at 8.4m/s wind speeds.
	3.2 Achieve maximum energy production	Produce 350 GW/year .
	3.3 Maximise turbine availability	Turbine should have 8322 hours/year of operational time.
	3.4 Maintain operational efficiency	Maintain efficiency levels within the target range of 40-50%. With current efficiency of design recorded at 40.6% .
4. Maintenance	4.1 Increase availability	Wind turbines should only be maintained for 5% of operation time.
	4.2 Equipment reliability	Routine inspections every 500 hours .

	4.3 Corrective maintenance	Perform on demand maintenance as needed on failed or worn components.
		Utilise modern equipment (vibration analysers and thermographic cameras) to diagnose root cause of failures.
		Conduct post-failure analysis to promote improvement in maintenance practices.
	4.4 Optimise remote condition monitoring	Utilise meteorological towers, LiDAR and radar systems to monitor weather.
		Mitigate ice buildup by installing a detection and de-icing system.
		Ensure lightening protection system is set in place to prevent blade damage.
	4.5 Maintain high levels of safety	Conduct risk assessment to predict and prevent potential risks to employees and environment.
		Install emergency shutdown mechanisms.
	5. Materials	5.1 High environmental compatibility
Material with high melting temperature to prevent damage due to lightening.		
Choose material inert to biohazards .		
Coat blade with epoxy coating to provide boundary layer control .		
5.2 Select material based on design requirements		Select lightweight materials with high strength and fatigue resistance.
5.3 Minimise environmental impact		Consider recycled materials where possible.
5.4 Minimise waste		Consider on-site waste treatment options to reduce volume of waste requiring disposal.
5.5 Conduct End-of-life planning		Design decommissioning and disposal of blades to be sustainable by contributing to the circular economy

2.3 / PROJECT MANAGEMENT

All members of the group underwent the Belbin test for role assignments [1]. The selection of the group leader was determined by both the identified roles and the individual's confidence level. The position of group leader entailed the allocation of tasks, strategising, liaising between groups, and conveying the team's broader objectives to the group's activities. Group leaders participated in in-person meetings to discuss overarching goals and inform other teams of progress and challenges. Meetings also involved reviewing individual progress, addressing issues, and delegating tasks to ensure deadlines were met; direct communication minimised the risk of misunderstandings.

WhatsApp [a] and Teams groups [b] were established to facilitate communication and file sharing, complemented by weekly meetings to track the project's progress. A OneDrive [c] was split into group folders which allowed work to be accessible by every member of the team. Bi-weekly sessions with the supervisor provided opportunities for inquiries and guidance, ensuring a cohesive and well-supported project development process. Tasks were then meticulously listed and allocated according to each member's strengths as shown in Table 2.

Table 2: Roles and tasks assigned to each member

Member	Role	Tasks assigned
Mahmood El-Mahalawy	Leader/ Co-ordinator	<ul style="list-style-type: none"> • Limitations and mitigation of blade • Final design assembly and part drawings • Calculations • Prototype • FEA
Zara Iman-Butt	Shaper	<ul style="list-style-type: none"> • Risk assessment and FMEA • Research of blades • Project Management • Ergonomic Evaluation • Final design assembly and part drawings • Prototype
Heba Ali	Plant	<ul style="list-style-type: none"> • CAD and CFD of concept designs • Final design CAD • Business plan- investment • Prototype
Shelly Tchoutezo	Specialist	<ul style="list-style-type: none"> • Materials selection and life cycle analysis • Business plan- Manufacturing
Sundus Abdirahin	Monitor Evaluator	<ul style="list-style-type: none"> • Calculations • Experimentation • FMEA • Justification of design • Operations list • Business plan- Market
Waddah Alowadh	Resource Investigator	<ul style="list-style-type: none"> • CAD and CFD of concept designs • Final design CAD • Bill of materials
Hoda Chahini	Completer Finisher	<ul style="list-style-type: none"> • PDS • Risk assessment • Assembly and manufacturing route sheet • Wider Engineering implications • Business plan-setting up the business and RoR

A Gantt chart shown in Figure 1 was utilised to facilitate the simultaneous completion of multiple tasks and track work progression to meet deadlines.

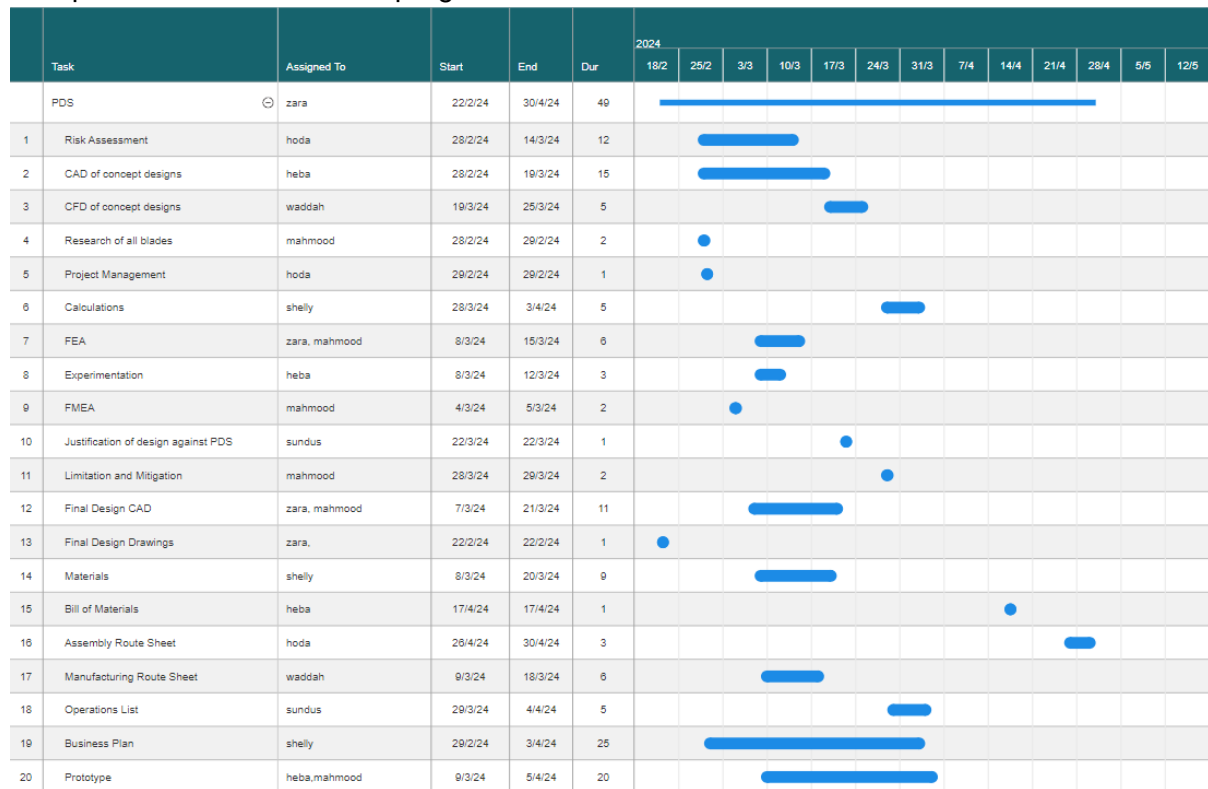


Figure 1: Gantt Chart of project development

To effectively manage the blade design sub-project within a fixed timeframe, a MUSCOW analysis was conducted to pinpoint essential targets. This approach enabled dynamic project management despite the deadline constraints. The analysis, detailed in Table 3, served as a tool for prioritising objectives and identifying critical tasks required for successful completion.

Table 3: MUSCOW analysis to prioritise tasks

Must	<ul style="list-style-type: none"> • Complete CAD and CFD • Complete calculations for blade speed/angle • Complete bills of materials • Complete FEA
Should	<ul style="list-style-type: none"> • Consider sustainability • Consider maintenance • Be designed for optimal balance and stability • Have low environmental impact in terms of manufacturing
Could	<ul style="list-style-type: none"> • Create simulations for blade angle and how it would impact speed • Look into future blade materials to reduce the maintenance • Include features for noise reduction
Would Not	<ul style="list-style-type: none"> • Consider patent • Prioritise aesthetic features over functional performance

Each meeting was recorded in Table 4. If a meeting could not happen in person it would be held online at a time suitable for majority of the group.

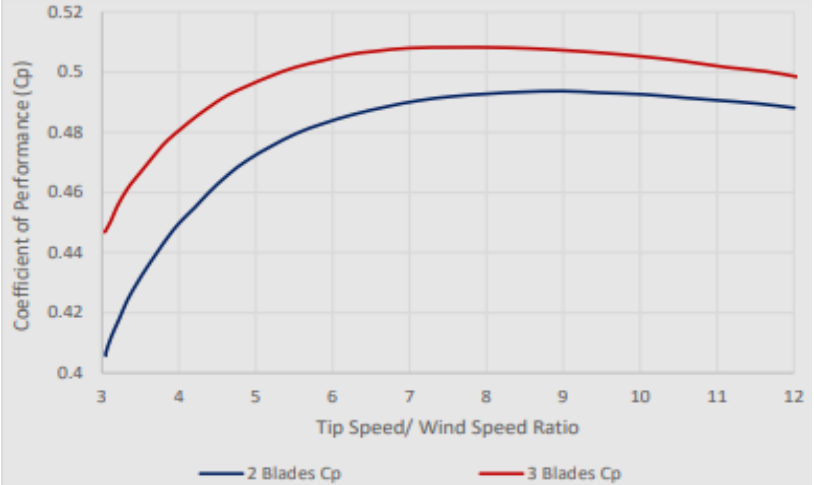
Table 4: List of Meetings

Date/ Meeting setting	Discussion	Outcome
1/03/24 In person meeting	<ul style="list-style-type: none"> The types of blades we could focus on. 	Each member to do research on blades.
4/03/24 In person meeting	<ul style="list-style-type: none"> What angles of blades that could be used. Discussed the engineering implications. 	Engineering implications were split up and assigned to each member.
7/03/24 In person meeting	<ul style="list-style-type: none"> Made a list of all the tasks for the report. 	Split the tasks up and used a Gantt chart.
14/03/24 In person meeting	<ul style="list-style-type: none"> The size of the blades and how it could impact the cost. What parameters to assume when doing the calculations. 	Decided on the size that would produce the most energy and the parameters assumed would be typical conditions of Crete.
22/03/24 In person meeting	<ul style="list-style-type: none"> What would get completed over the Easter break and deadlines for the tasks. 	Everyone had a clear task overview for the next few weeks and the individuals working together on tasks could meet during the break.
5/04/24 Online meeting	<ul style="list-style-type: none"> Update with progress of individual tasks Advise/help needed on certain tasks were asked 	New tasks were able to be started. Solutions to problems were made.
19/04/24 Online meeting	<ul style="list-style-type: none"> Went through everyone sections and discussed what could be added/improved 	Improvements made were able to be implemented.
25/04/24 In person meeting	<ul style="list-style-type: none"> Discussed feedback from supervisor 	Made further improvements.
29/04/24 In person meeting	<ul style="list-style-type: none"> Discussed how the report should be formatted and presented 	Formatted the report together and made last changes.

2.4 / RESEARCH

To generate concept designs for turbine blades, all potential designs were thoroughly assessed and selected according to their suitability for the energy island's requirements. Below the different considerations are discussed and justified in Table 5 and 6.

Table 5: Research for optimum blade design

Area of Research	Finding	Justification
Number of Blades	A horizontal -axis design featuring 3 blades is regarded as the most efficient [2]	<p>This arrangement provides a balance of gyroscopic forces and produces less noise in comparison to alternative designs. Figure 2 depicts the comparison between a two-blade and a three-blade wind turbine.</p>  <p>Figure 2: Power coefficient versus tip speed of two bladed and three bladed wind turbines.</p> <p>From Figure 2, it is evident that the coefficient of performance is higher for a 3-blade turbine than for a 2-blade turbine. A greater coefficient of performance indicates greater efficiency in converting wind energy into electrical power.</p>
Blade Shape	Two main types of blades used in industry are twisted and tapered blades	These blades have optimised aerodynamic efficiency, reduced noise/vibration, and can adapt to changes in wind direction/speed [3]. To evaluate which of these shapes would be best for the energy island 3 shapes were designed- twisted, tapered and twisted with tapered.
Angle of Twist	Wider angle of twist used in industry	The angle of twist underwent optimisation through CFD simulations, as this angle varies depending on the specific requirements and constraints of each turbine design. Research focused on offshore wind turbines revealed that a wider angle of twist facilitated efficient energy capture irrespective of wind direction or intensity. Consequently, a twist angle ranging from -2.5 to 20 degrees was selected for these reasons [4].
Angle of Taper	Angle of 10 degrees most optimal	The angle of taper defines the gradual narrowing of the blade from its root to its tip. While the typical industry standard ranges from 3 to 8 degrees, research has revealed that for the specific environmental conditions, characterised by variable wind speeds, an angle of 10 degrees most optimal. This adjustment

		enhances the structural integrity of the design, a critical factor given the extreme weather conditions in which the wind turbines will operate [5].
Lift to Drag Ratio	High lift to drag ratio is more efficient	The lift-to-drag ratio serves as a crucial measure of aerodynamic efficiency. In general, a high lift-to-drag ratio is desirable as it indicates that the blade is generating more lift, which contributes to enhanced energy capture. To evaluate the effectiveness of different blade designs, drag ratios of 4, 10, and 39 were compared [6].

Table 6: Research for calculations section

Area of Research	Finding	Justification
Turbine Efficiency	Range of 30%-45 %	Modern commercial wind turbines often have efficiency ranging from 30% to 45% depending on size and wind speed at the location [7]. Offshore wind turbines typically have a higher efficiency and so 45% was assumed in section 2.6.2.
Mechanical Efficiency	Range of 95%-98%.	Offshore wind turbines have a mechanical efficiency range from 95% to 98%. The following Table 5 lists the assumptions made during the CFD and FEA. These assumptions had potential risks which were mitigated in the design and manufacturing of the components [7]. An efficiency of 96% was chosen based on this.
DU Airfoils	Several airfoils with high lift to drag ratios was most optimum	DU40_A17, DU35_A17, DU30_A17, DU25_A17, DU20_A1 are the airfoils part of the DU (Delft University) series, which are well-known and widely used in aerodynamic research and wind turbine blade design. They are characterized by favourable lift-to-drag ratios, good stall characteristics, and low sensitivity to roughness, making them suitable for various wind conditions and blade designs [8].
NACA Airfoils	High lift coefficient for tip	NACA64_A17 : The NACA 6-series airfoils, including the NACA64_A17, have been extensively studied and used in aircraft and wind turbine applications. These airfoils offer a balance between lift and drag, with relatively high lift coefficients and favourable stall behaviour. They have been adapted and optimized for wind turbine blades to improve energy capture and overall turbine efficiency [9].
Deflection of blades	Low value of 2.52×10^{-6} m for flapwise and 4.15×10^{-6} m for edgewise	GFRP blades commonly demonstrate minimal deflection, as evidenced by the relatively low value of 2.52×10^{-6} m for flapwise deflection. This is attributed to the engineered stiffness and structural integrity of GFRP materials, which mitigate deformation when subjected to external forces. Although balsa wood boasts commendable stiffness and strength attributes, it lacks the rigidity of GFRP composites, resulting in potentially higher deflection values when under load. The provided figure of 4.15×10^{-6} m for edgewise deflection likely reflects characteristics inherent to balsa wood cores or components within composite blades [10].
Length of Shaft	10 m shaft optimum	A 10-meter shaft length for the wind turbine was chosen based on factors like tower height, structural stability, drive train configuration, manufacturing feasibility, transportation logistics, and cost-effectiveness [11].

2.5 / CONCEPT DESIGNS

To determine the optimal blade design, a CFD analysis was conducted, using ANSYS CFX [d], evaluating three prominent blade variants commonly used in industrial applications: the tapered, twisted, and a combination of twisted and tapered blades. This analysis determined their respective efficiencies and performance characteristics. By examining these variants through CFD simulations, insights into their aerodynamic behaviour can be compared. Figure 3 illustrates the process that was followed in the CFD analysis.



Figure 3: Flow chart of CFD steps

The turbulence model was set as k-epsilon as it is a robust option for a wide range of turbulent flow situations and offers a good compromise between accuracy and computational efficiency.

Boundary conditions play a critical role in CFD simulations, affecting the accuracy and reliability of the results. They must be specified to define how a system interacts with its surroundings and solve both ordinary and partial differential equations. Table 7 outlines the boundary conditions used.

Table 7: Boundary conditions and justification

Boundary	Condition	Justification
Inlet	Wind speed of 8.4 m/s	Based on the yearly average wind speed in Crete at 100 m above sea level.
Outlet	Atmospheric pressure	Average air pressure which mimics natural conditions of wind turbine.
Blade Surface	No-slip wall	Velocity of air at the blade surface is zero. Ensures blade has roughness for a proper boundary layer profile. Allows for surface shear stresses and viscous drag to be accounted for.
Rotational Domain	Rotational speed of 9.5 rpm	Calculated in section 2.6.2 based on wind speed and pitch angle.

Table 8 lists the assumptions made in the CFD set up and the limitations created. The effect of the limitations can limit the scope and accuracy of the results. However, they were necessary for simplifying complex phenomena, making problems tractable with the available computational resources.

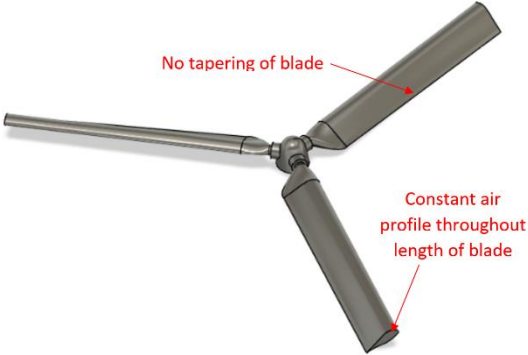
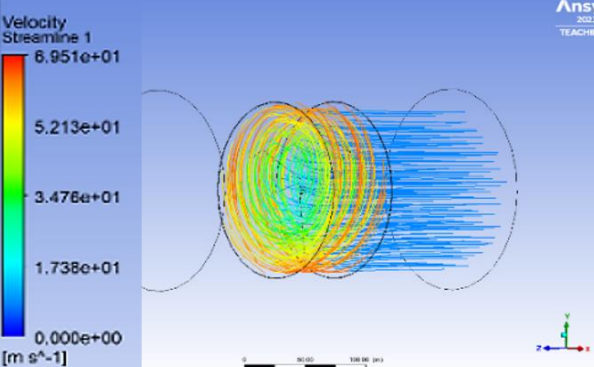
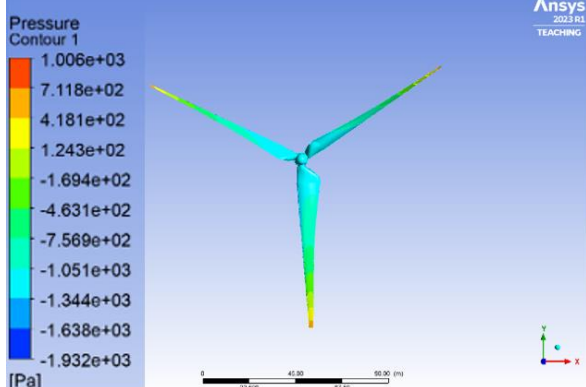
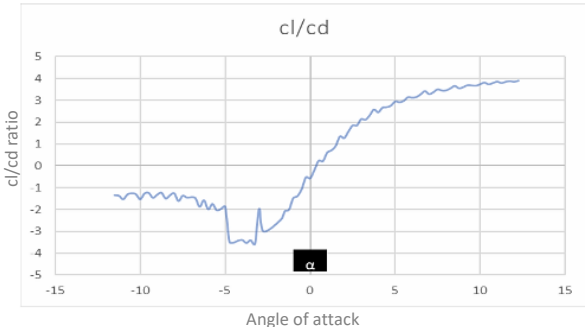
Table 8: Boundary conditions and justifications

Assumptions	Limitations
Steady flow	Flow is assumed to be steady to reduce computational resources but ignores transient effects.
Incompressible flow	Overlooks density variations which could be significant at higher speeds.
Isotropic turbulence	Does not consider anisotropic behaviours which usually occur near boundaries and wake regions.
Perfect gas law	Assumes constant thermodynamic properties which is not accurate when temperature and pressures vary.

The mesh density was strategically reduced to manage computational demands. While a finer mesh would enhance the accuracy by improving the resolving fluid dynamics near complex geometries, the increased computational cost exceeds the current processing capabilities.

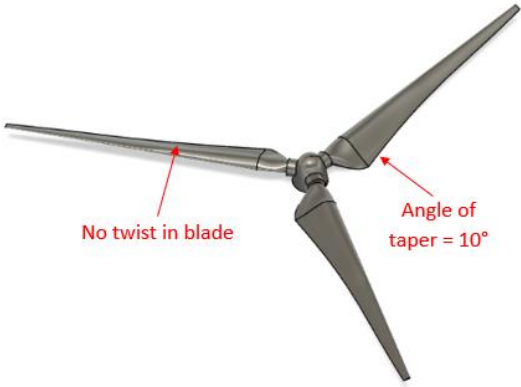
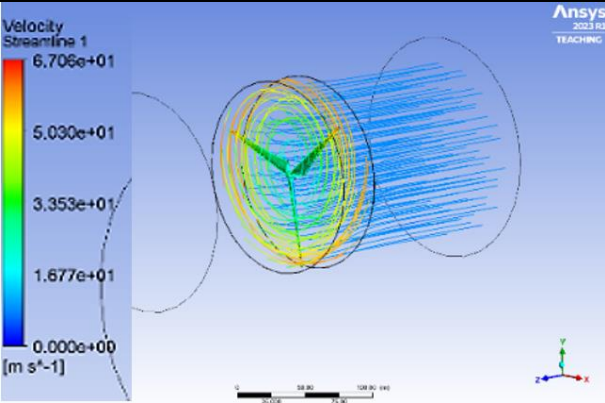
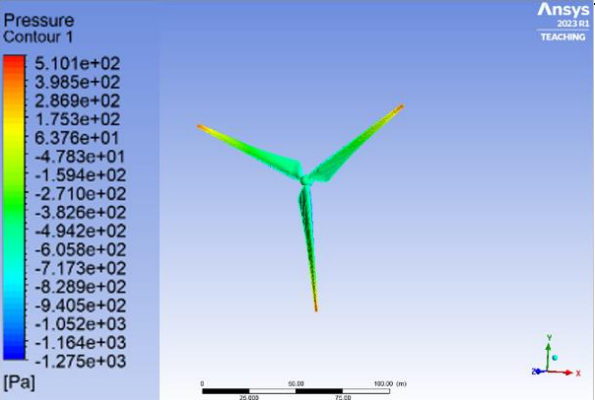
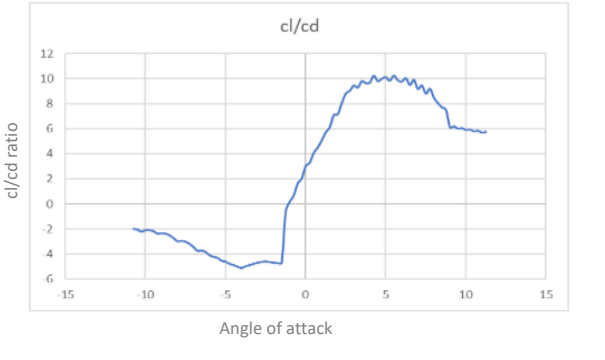
Table 9 illustrates the key features that were analysed for the twisted blade with an overview of what was concluded from the analysis.

Table 9: Geometry and CFD analysis for twisted blade concept design

Twisted Blade	
 <p>Figure 4: CAD model of twisted blade</p>	 <p>Figure 5: Velocity profile of twisted blade</p>
<ul style="list-style-type: none"> • Uniform width from root to tip. • Single airfoil used along full length of blade. • Angle of twist ranging from -2.5 degrees to 20 degrees. • Produces greater lift in comparison to tapered blade due to twist angle. 	<ul style="list-style-type: none"> • Airflow speed varies significantly across span of blade. • Coiling of streamlines indicates twist increases efficiency. • Higher velocities at blade tips. • Design equalises lift distribution reducing bending moments.
 <p>Figure 6: Pressure contour of twisted blade</p>	 <p>Figure 7: Coefficient of lift to drag ratio for twisted blade</p>
<ul style="list-style-type: none"> • Highest pressures act at the tip of the blade and on windward side. • Lowest pressures act at the hub and on the leeward side (away from the wind). • Produces the least significant pressure gradient of the three blades indicating there will be more turbulence and vortices. 	<ul style="list-style-type: none"> • The twisted blade had the smallest maximum coefficient of lift to drag ratio for varying angles of attack. • Beyond 0 degrees the efficiency decreases due to flow separation or stall.

The second concept design selected was a tapered blade, which is more commonly used in industry. Similar to the previous table, Table 10 offers an analysis of the key features obtained from the CFD analysis.

Table 10: Geometry and CFD analysis for twisted blade concept

Tapered Blade	
 <p>Figure 8: CAD model of tapered blade</p>	 <p>Figure 9: Velocity profile of tapered blade</p>
<ul style="list-style-type: none"> • Blade narrows from root to tip by 10 degrees. • Offers a reduced mass and moment of inertia at the blade tips. • Tapering reduces blades resistance to bending which lowers material stress and increases lifespan. 	<ul style="list-style-type: none"> • Increased uniformity compared to twisted blade. • Streamlines are less coiled indicating air flow is less distributed by blades geometry.
 <p>Figure 10: Pressure contour of tapered blade</p>	 <p>Figure 11: Coefficient of lift to drag ratio for tapered blade</p>
<ul style="list-style-type: none"> • Greater pressure distribution towards tip compared to twisted blade due to decreased surface area and lower aerodynamic forces at this point. 	<ul style="list-style-type: none"> • Beyond -2 degrees the coefficient of lift to drag ratio increases up until 5 degrees. • These are the optimal values for the angle of attack. • Beyond the optimal region the ratio maintains high values reflecting the blades ability to maintain performance.

The final concept design, shown in Table 11 was an amalgamation of the previous two concepts. It was selected as the first two concepts offered individual benefits so it was assumed that combining geometric features would improve the overall efficiency of the blade.

Table 11: Geometry and CFD analysis for twisted and tapered blade

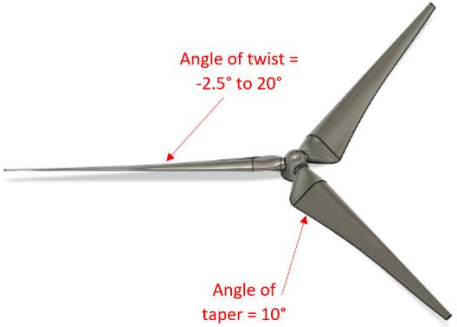
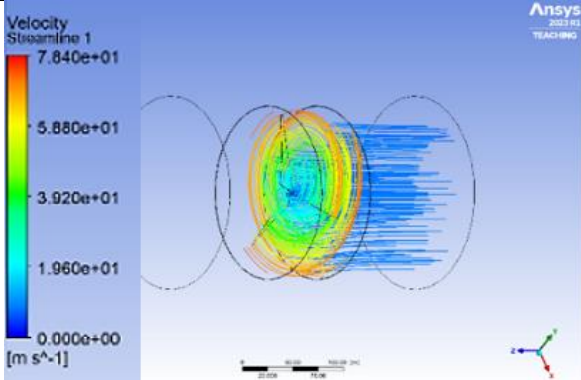
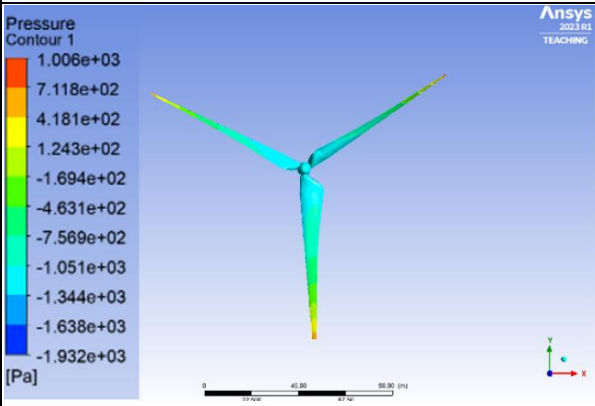
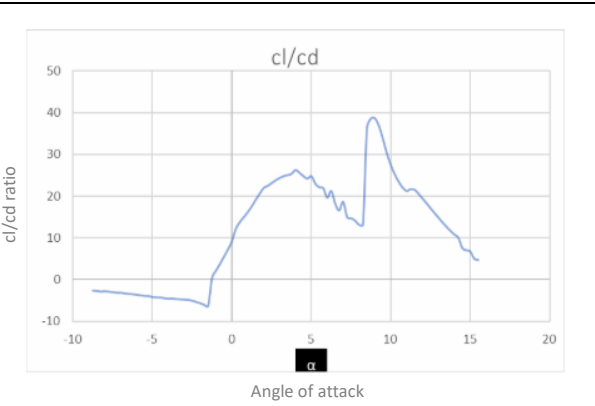
Twisted and Tapered Blade	
 <p>Figure 12: CAD model of twisted and tapered blade</p>	 <p>Figure 13: Velocity profile of twisted and tapered blade</p>
<ul style="list-style-type: none"> • Twist allows each section to meet the wind at an optimal angle of attack to capture the most energy. • Taper decreases the material at the tip which decreases stress concentrations improving durability. It also reduces cost. 	<ul style="list-style-type: none"> • Streamlines amalgamate effects of the blades shown in Figure 1 and 3. • Coiled streamlines indicate twist is increasing rotational velocity. • Uniformity of flow is from tapered aspect of blade.
 <p>Figure 14: Pressure contour of twisted and tapered blade</p>	 <p>Figure 15: Coefficient of lift to drag ratio for twisted and tapered blade</p>
<ul style="list-style-type: none"> • Pressure distribution for combined tapered and twisted blade is the greatest. • Smooth gradient from root to top indicating efficient aerodynamic performance. 	<ul style="list-style-type: none"> • Multiple and broader peaks for optimal angles of attack which means blade can perform efficiently over a wider range if wind conditions. • Highest coefficient of lift to drag ratio of the three concept designs.

Table 12 shows the values obtained from the CFD analysis for the torque and maximum lift/drag coefficient. The twisted and tapered blade offers the highest torque which implies a greater force turns the rotor resulting in more power being generated. It also has the highest lift/drag coefficient meaning the blades are more effective at converting wind energy into rotational energy.

Table 12: Data obtained from CFD for each blade variant

	Twisted	Tapered	Twisted and Tapered
Torque (Nm)	6.86×10^6	2.76×10^6	7.43×10^6
Max lift/drag coefficient	4	10	39

2.6 / TECHNICAL EVALUATION OF FINAL DESIGN

2.6.1 / Ergonomic Evaluation

During the design phase, the ergonomics of the wind turbine blade components was prioritised, to simplify both assembly and maintenance tasks. Table 13 goes through the different features.

Table 13: Ergonomic features of the turbine

Features	Description
Accessibility	Platforms or mechanisms for safe and convenient access to different areas of the blade.
	Easily accessible ports or panels along the shaft for inspection of internal components, such as bearings and gears.
	Provide alignment guides or markings to assist workers in aligning shaft components accurately during assembly.
Safety Features	Presence of safety mechanisms such as guardrails, harness attachment points, and warning signs.
	Implement locking mechanisms to secure the shaft during maintenance, preventing accidental rotation.
	Provide emergency override systems to quickly adjust the pitch of the blades in case of unexpected events or malfunctions.
Maintenance procedures	Ensure bolts are easily accessible for maintenance and assembly.
	Position parts correctly to prevent damage to neighbouring components during assembly.
	Blades designed so that individual sections can be replaced.
Environmental	Temperature, wind, and precipitation on worker comfort, safety, and performance has been considered by providing portable shelters.
	Evaluate the levels of noise and vibration generated by the turbine and assess their potential effects on worker health, provide ear defenders.



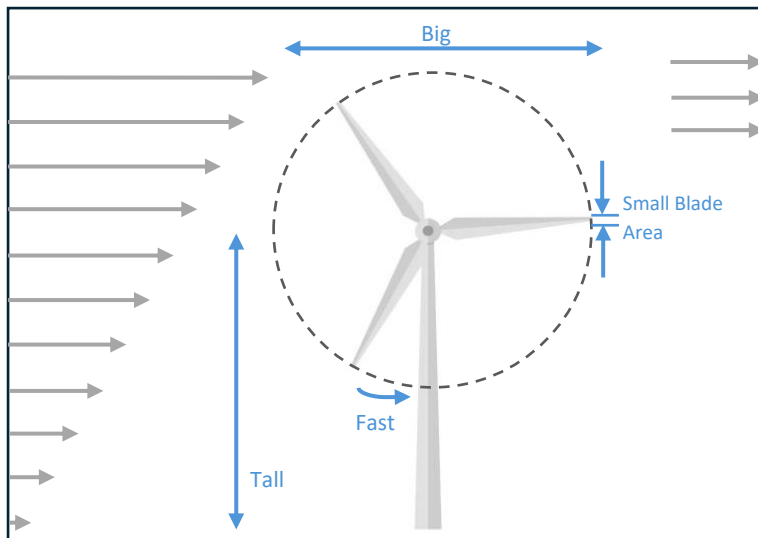
Figure 16: Turbine with guardrails [12]



Figure 17: Attachment system on ladders [12]

Physics of Wind Turbines:

Turbines catch the wind's energy with their propeller-like blades, which act much like an airplane wing as the blades have an airfoil shape. When the wind blows, a pocket of low-pressure air forms on one side of the blade and this low-pressure air pocket then pulls the blade toward it which causes the rotor to turn. This creates the force of lift. The force of the lift is much stronger than the wind's force against the front side of the blade which is the force of drag. The combination of lift and drag causes the rotor to spin and generate power.



The wind turbine needs to be:

- Big to capture a lot of wind for more power production
- Tall to capture strong winds
- Fast moving to be most efficient
- Narrow bladed since fast moving turbines need smaller blade area to not slow down the wind too much

Figure 18: Wind turbine diagram

General Assumptions:

Table 14 outlines basic assumptions for specific parameters essential for blade design calculations, along with their justifications.

Table 14: Justification for parameter assumptions

Notation	Parameter	Value	Unit	Reason For Assumption
n	No. of Blades	3	-	Switching from a 2-blade to a 3-blade propeller design improves aerodynamic efficiency by about 3%, while moving to a 4-blade design offers a minimal 0.5% gain. Given the significant cost increase with more blades, a 3-blade design is considered ideal, utilising blades with a thicker root for better resistance to axial wind loads [4].
V	Wind Speed	8.4	m/s	Wind speed was based on turbine tower height at 100m off the west coast of Crete.
t	Time	8322	hrs	This represents the turbine's operational time over the year (8760 hrs), factoring in periods for maintenance.
r	Blade Radius	60	m	This blade was chosen to ensure ease of manufacturability and transport as well as being cost effective.

Power and Energy:

Power and Energy need to be calculated to calculate other parameters such as rotational speed of the blades and number of turbines. To calculate the power extracted of the wind turbine by the wind, the efficiency of the turbine and the power of the wind need to be calculated. The overall turbine efficiency shown in Figure 19 is calculated by multiplying the different efficiencies throughout the turbine. This includes turbine efficiency (efficiency with which the blades convert available wind power to rotating shaft energy), mechanical efficiency (efficiency through the bearings and gear tooth friction) and electrical efficiency (efficiency of the generator).

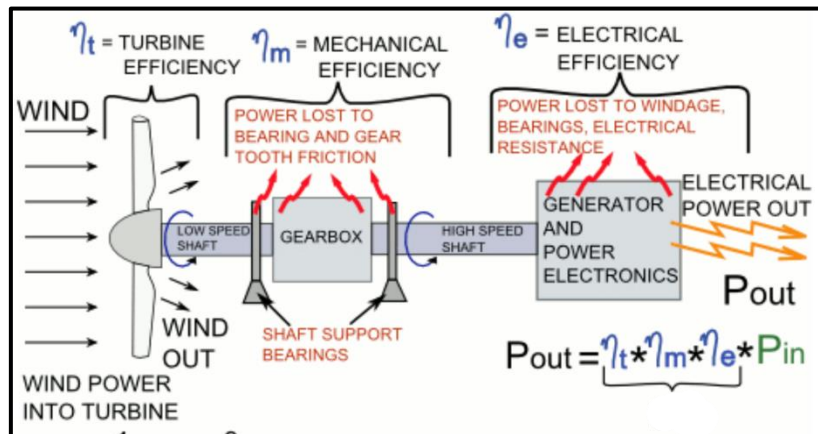


Figure 19: Efficiency throughout the wind turbine [13]

The average values for these efficiencies were found to be:

- Turbine efficiency, $\eta_t = 0.45$
- Mechanical efficiency, $\eta_m = 0.96$
- Electrical efficiency, $\eta_e = 0.94$

$$\eta = \eta_t \times \eta_m \times \eta_e = 40.6\% \quad (1)$$

In order to determine if this is a high efficiency it needs to be compared to the Betz efficiency, η_{betz} , as shown in Equation 2. The Betz efficiency is a theoretical limit that dictates the maximum efficiency achievable by any wind turbine and states that no wind turbine can capture more than 59.3% of the kinetic energy in wind.

$$\frac{\eta}{\eta_{betz}} = \frac{0.406}{0.59} = 68.8\% \quad (2)$$

The efficiency came out to be 68.8% which is the efficiency that the wind turbine can achieve in practical terms by factoring into account real-world conditions.

The power of the wind needed to be calculated at a speed of 8.4m/s. This was the average wind speed at 100m off the west coast of Crete. Area was calculated as 11304m² which was done based of a 60m blade radius and is shown in Table 15.

$$P_{wind} = \frac{\rho A V_1^3}{2} \quad (3)$$

Table 15: Parameters used to calculate Wind Power

Notation	Parameter	Value	Unit
ρ	Air Density	1.225	kg/m ³
A	Area of Turbine	11304	m ²
V	Wind Speed	8.4	m/s
P_{wind}	Wind Power	4.02	MW

With the efficiency and wind power calculated, the power extracted in Table 16 can now be calculated using Equation 4.

$$P_{extracted} = P_{wind} \times \eta = 0.688 \times 4.02 \times 10^6 = 1.63 \times 10^6 \text{ W} \quad (4)$$

Table 16: Parameters used to calculate Extracted

Notation	Parameter	Value	Unit
P_{wind}	Wind Power	4.02	MW
H	Total turbine Efficiency	0.406	-
$P_{extracted}$	Extracted Power	1.63	MW

The power extracted was found to be 1.63×10^6 W. This needs to be converted to energy to work out the required number of wind turbines for the island. Assuming the total number of hours the wind turbines are operational for is 8322 hours, the total energy produced can be calculated using equation 5.

$$Energy = P_{extracted} \times \text{time} = 1.63 \times 10^6 \times 8322 = 13.6 \text{ GWh/yr} \quad (5)$$

This is the energy produced for one turbine. Since the wind turbines will be producing 70% of the island's energy, this will mean 350 GWh/yr needs to be produced by the turbines. In total this would mean the island requires **26 wind turbines**.

Blade Aerodynamic Design:

An essential aspect of blade aerodynamic design is the angle of attack of the airfoil, which significantly influences both the lift coefficient and the drag coefficient. Ideally, the design should maximise the lift-to-drag ratio, L/D, allowing the wind turbine to achieve maximum lift with minimal resistance. Figure 20 demonstrates that the optimal L/D ratio occurs between angles of attack of 6° to 9°. Figure 21 illustrates how various airfoil shapes affect the lift coefficient, with all shapes converging at an angle of attack of approximately 5°, producing a lift coefficient of 1. Consequently, the optimum angle of attack was chosen to be 6.5°.

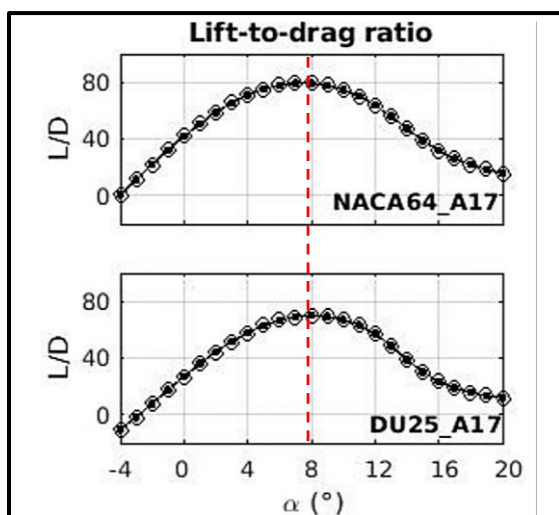


Figure 20: Angle of attack against L/D ratio for airfoils used in the blade [14]

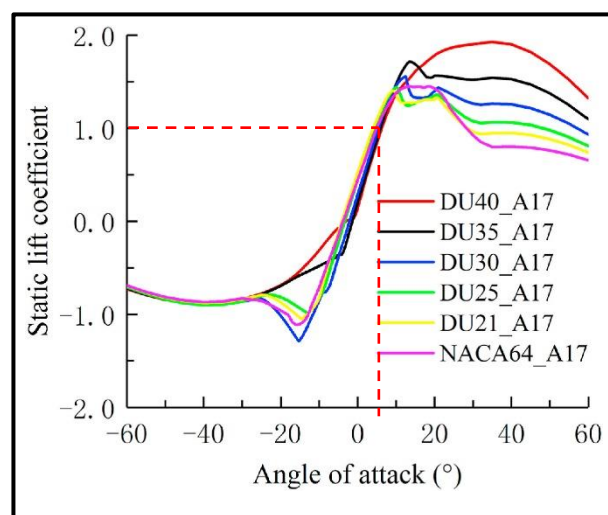


Figure 21: Angle of attack against static lift coefficient for all airfoils [15]

Lift force is created due to the airfoil shape along the blade. The different airfoil profiles along a wind turbine blade are designed to address the varying aerodynamic demands from the root to the tip. This variation is necessary because wind speed increases with height, meaning that the outer sections of the blade encounter higher wind speeds than those closer to the root. Consequently, airfoils towards the tip are optimised for performance at higher speeds and lower loads, often being thinner and more aerodynamically refined. In contrast, airfoils near the root are thicker and sturdier to withstand greater mechanical stresses and support the weight of the blade. This variation in airfoil profiles helps optimise the blade's overall efficiency and durability, ensuring it achieves the best possible performance across its entire length. Figure 22 shows the variation of airfoil profiles used along the blade.

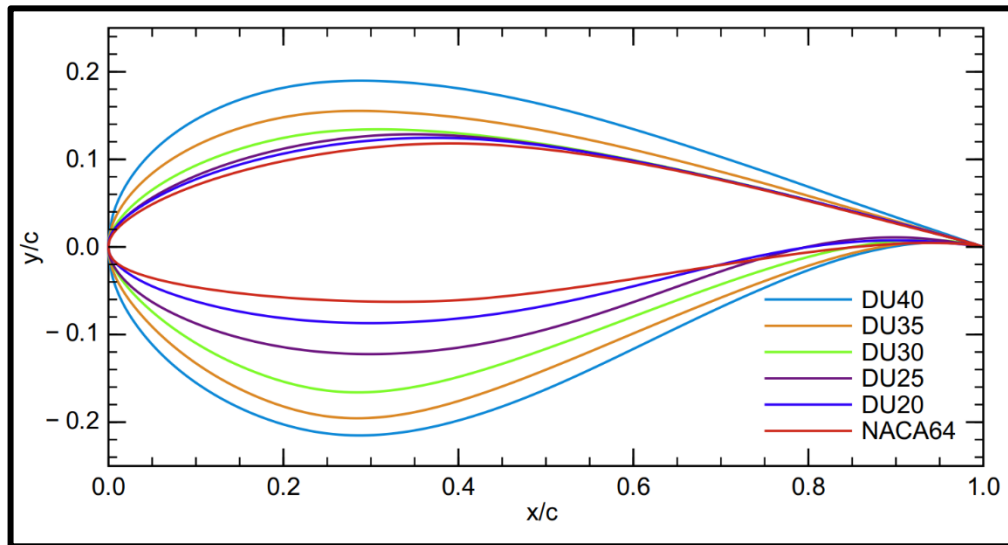


Figure 22: Range of airfoils used in blade in comparison to each other [16]
 Wind turbine blades need to capture the maximum amount of energy from the wind. This section looks at calculating parameters such as the chord length, rotational speed and different blade angles in Table 17 required for the optimum design of the blade.

$$RPM, U = \frac{V}{\tan\theta} * \frac{180}{\pi} \quad (6) \quad RPM, \Omega = \frac{U}{r} * \frac{2\pi}{60} \quad (7)$$

Table 17: Parameters used to calculate Rotational Speed

Notation	Parameter	Value	Unit
R	Blade Radius	60	m
θ	Pitch Angle	8	deg
V	Wind Speed	8.4	m/s
RPM, U	Relative velocity	59.9	m/s
RPM, Ω	Rotational speed	9.51	rpm

Tip Speed ratio in Table 18, as seen in equation 8, needs to be calculated to compute the chord length of each airfoil at every section of the blade.

$$\lambda = \frac{\Omega r}{V} \quad (8)$$

Table 18: Parameters used to calculate Tip Speed Ratio

Notation	Parameter	Value	Unit
Ω	RPM	9.51	rpm
r	Blade Radius	60	M
V	Wind Speed	8.4	m/s
λ	Tip Speed Ratio	7.12	-

Chord length is a critical component in the design of the blade and affects the aerodynamic performance of the blade. The chord length varies along the length of the blade; wider at the root of the blade and tapers towards the tip. Equation 9 gives the equation to calculate the chord length at various points along the blade with the twist angle being shown in Table 19.

$$C = \frac{16\pi R^2}{9nC_L r \lambda^2} \quad (9)$$

Table 19: Chord length and twist angle along radius of blade

Section	Radius (m)	Chord Length (m)	Twist Angle (°)	Airfoil
1	3	3.00	0	Cylinder Foil
2	6	3.00	0	Cylinder Foil
3	9	4.63	0	Cylinder Foil
4	12	5.12	7	DU40_A17
5	15	5.75	10	DU40_A17
6	18	6.08	20	DU35_A17
7	21	5.21	18	DU35_A17
8	24	4.56	14	DU30_A17
9	27	4.05	12	DU30_A17
10	30	3.65	8	DU25_A17
11	33	3.32	5	DU25_A17
12	36	3.04	3	DU20_A17
13	39	2.81	2	DU20_A17
14	42	2.60	1	NACA64_A17
15	45	2.43	0.2	NACA64_A17
16	48	2.28	0	NACA64_A17
17	51	2.15	-1	NACA64_A17
18	54	2.03	-1.5	NACA64_A17
19	57	1.92	-2	NACA64_A17
20	60	1.82	-2.5	NACA64_A17

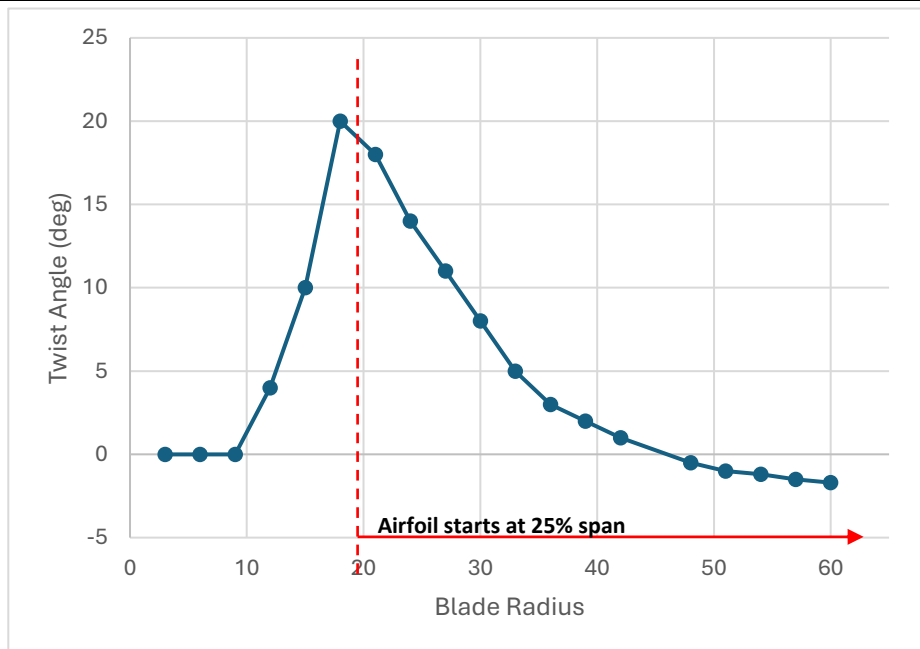


Figure 23: Twist angle along span of the blade

Figure 23 shows the change in twist angle along the blade. The maximum angle starts at 18 m which is 25% of the span on the blade radius.

Aerodynamic Forces:

The lift (Equation 10) and drag (Equation 11) of the blade's aerofoil section creates aerodynamic forces, which acts on the flapwise direction of the blade (Figure 24). These were calculated using the blade element momentum (BEM) theory [17] to calculate the resultant aerodynamic force (Equation 12) as shown in Table 20.

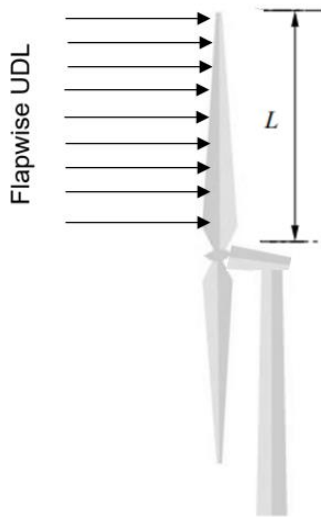


Figure 24: Flapwise load acting on blade

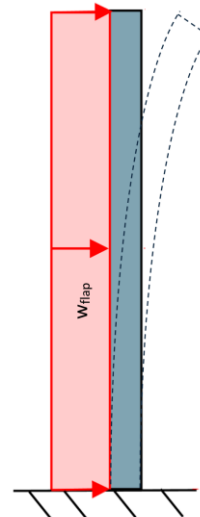


Figure 25: Blade modelled as cantilever beam with flapwise load

$$F_L = \frac{1}{2} C_L \rho v^2 A \quad (10)$$

$$F_D = \frac{1}{2} C_D \rho v^2 A \quad (11)$$

$$F_{flap} = \sqrt{F_L^2 + F_D^2} \quad (12)$$

Table 20: Parameters used to calculate the resultant flap wise load

Notation	Parameter	Value	Unit
C_L	Lift coefficient from graph x	1.2	-
C_D	Drag coefficient from graph x	0.015	-
ρ	Air Density at 20°	1.225	kg/m ³
v	Wind speed	8.4	m/s
A	Blade swept area	11304	m ²
F_L	Lift force	591	kN
F_D	Drag force	440	kN
F_{flap}	Resultant flapwise force	737	kN

Gravitational and Centrifugal Forces:

Due to the rotor diameter being 120 m, the gravitational (Equation 14) and centrifugal forces (Equation 13) are critical as they depend on the mass, generally increasing cubically with turbine diameter [17]. The resultant of these two forces (Equation 15) acts on the edgewise direction of the blade (Figure 26) and is shown in Table 21.

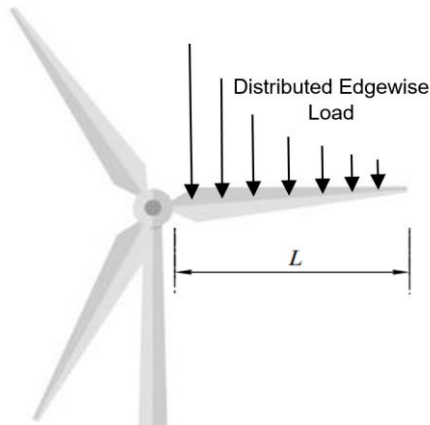


Figure 26: Edgewise load acting on blade

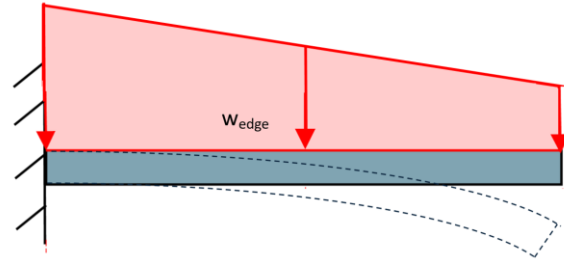


Figure 27: Blade modelled as cantilever beam with edgewise load

$$F_C = m\omega^2 r \quad (13)$$

$$F_G = mg \quad (14)$$

$$F_{edge} = \sqrt{F_{cent}^2 + F_w^2} \quad (15)$$

Table 21: Parameters used to calculate the resultant edgewise load

Notation	Parameter	Value	Unit
m	Mass of blade	98960	kg
ω	Rotational blade velocity	0.104	rad/s
r	Length of blade	60	m
g	Gravity	9.81	m/s ²
F_C	Centrifugal force	64.6	kN
F_G	Gravitational force	971	kN
F_{edge}	Resultant edgewise force	973	kN

Bending Moments and Deflection:

The blade was modelled as a cantilever beam (Figures 25 and 27) for the bending moment and deflection calculations with a uniformly distributed load (UDL) (Equations 16 and 17) for both the flapwise and edgewise directions shown in Table 22.

$$w_{flap} = \frac{F_{flap}}{r} \quad (16)$$

$$w_{edge} = \frac{F_{edge}}{r} \quad (17)$$

Table 22: Parameters used to calculate the flapwise and edgewise UDL's

Notation	Parameter	Value	Unit
F_{flap}	Resultant flapwise force	737	kN
F_{edge}	Resultant edgewise force	973	kN
r	Radius of blade	60	m
w_{flap}	UDL in flapwise direction	9.77	kN/m
w_{edge}	UDL in edgewise direction	16.22	kN/m

The flapwise deflection (Eq 18) and bending (Eq 20) occurs about the xx axis, whereas the edgewise deflection (Eq 19) and bending (Eq 22) occurs about the yy axis and are shown in Table 23. The values for the mass and area moment of inertia were found from the CAD model.

The Youngs Modulus of Epoxy/E-glass fibre was obtained from Ansys Granta EduPack. The maximum flapwise and edgewise deflections were both very low due to the assumptions outlined in Table 25. FEA was carried out to gain a more reliable result for the maximum deflection to determine if it was safe for the loads applied. The free body, bending moment and shear force diagrams are found in Figures 28 and 29 and show that the maximum bending moment and shear force occurs at the root and decreases towards the tip.

$$\delta_{max,flap} = \frac{w_{flap}r^4}{8EI_{xx}} \quad (18)$$

$$\delta_{max,edge} = \frac{w_{edge}r^4}{8EI_{yy}} \quad (19)$$

$$M_{max,flap} = \frac{1}{2}w_{flap}r^2 \quad (20)$$

$$M_{max,edge} = \frac{1}{2}w_{edge}r^2 \quad (22)$$

Table 23: Parameters used to calculate the maximum flapwise and edgewise deflection, bending, and shear force UDL's

Notation	Parameter	Value	Unit
w_{flap}	UDL in flapwise direction	9.77	kN/m
w_{edge}	UDL in edgewise direction	16.22	kN/m
r	Radius of blade	60	m
E	Youngs Modulus of Epoxy/E-glass fibre	40	GPa
I_{xx}	Area Moment of Inertia – xx axis	157,166	m ⁴
I_{yy}	Area Moment of Inertia – yy axis	158,320	m ⁴
$\delta_{max,flap}$	Maximum flapwise deflection	2.52×10^{-6}	m
$\delta_{max,edge}$	Maximum edgewise deflection	4.15×10^{-6}	m
$M_{max,flap}$	Maximum flapwise bending	17,600	kNm
$M_{max,edge}$	Maximum edgewise bending	29,200	kNm
$V_{max,flap}$	Maximum flapwise shear force	586	kN
$V_{max,edge}$	Maximum edgewise shear force	973	kN

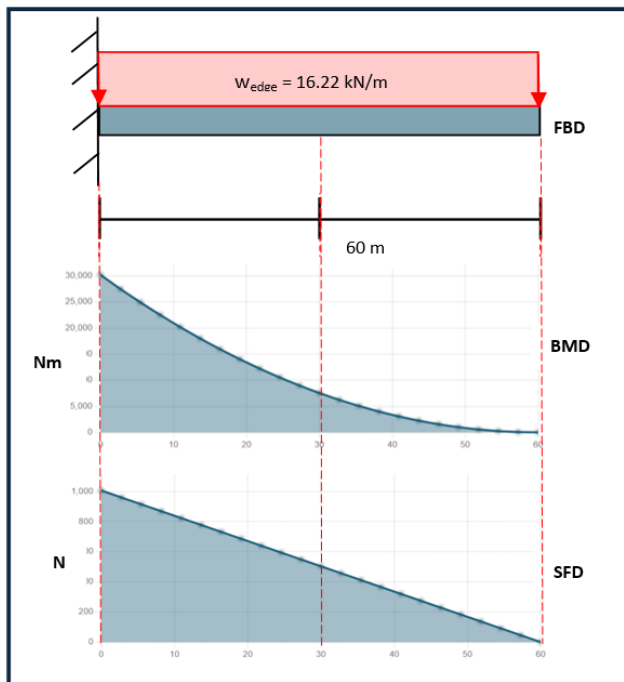


Figure 28: Edgewise free body, bending moment and shear force diagrams [g]

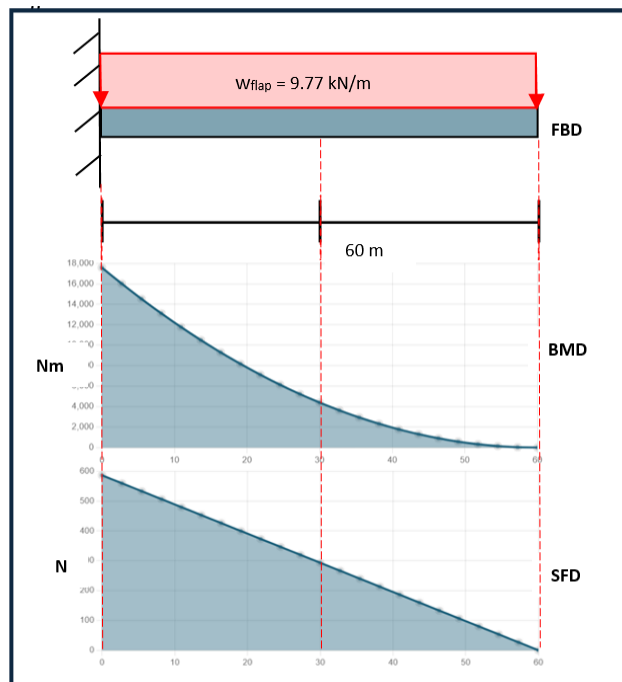


Figure 29: Flapwise free body, bending moment and shear force diagrams [g]

The maximum bending stress (Equations 23 and 24) and factor of safety (Equation 25) were calculated to ensure it was below the yield stress of both Epoxy/E-glass fibre and balsa wood so that it wouldn't fail. The factor of safety for both materials was very high meaning the design is safe for the loads it is subjected to.

$$\sigma_{max,flap} = \frac{M_{max,flap}r}{I_{xx}} \quad (23) \qquad \sigma_{max,edge} = \frac{M_{max,edge}r}{I_{yy}} \quad (24)$$

$$FOS = \frac{S_y}{\sigma_{max}} \quad (25)$$

Table 24: Parameters used to calculate the maximum flapwise and edgewise bending stress and Factor of Safety (FOS)

Notation	Parameter	Value	Unit
$M_{max,flap}$	Maximum flapwise bending moment	17,600	kNm
$M_{max,edge}$	Maximum edgewise bending moment	29,200	kNm
r	Radius of blade	60	m
I_{xx}	Area Moment of Inertia – xx axis	157,166	m ⁴
I_{yy}	Area Moment of Inertia – yy axis	158,320	m ⁴
$S_{y, glass-fibre}$	Yield strength of Epoxy/E-glass fibre	700	MPa
$S_{y, balsa-wood}$	Yield strength of balsa wood	18	MPa
$\sigma_{max,flap}$	Maximum flapwise bending stress	0.067	MPa
$\sigma_{max,edge}$	Maximum edgewise bending stress	0.11	MPa
$FOS_{glass-fibre}$	Factor of safety of Epoxy/E-glass fibre	6363	-
$FOS_{balsa-wood}$	Factor of safety of balsa wood	164	-

Table 25: Assumptions and limitations of the bending moment and deflection

Assumptions	Limitations	Mitigation
Blade modelled as a cantilever beam	Doesn't account for twist of the blade and neglects local stress concentrations	Using FEA, the complex geometry of the blade with the twists will give more accurate results and can capture stress concentrations as well as results for the internal structure of the blade
Uniformly distributed load applied	Wind loads change along the length of the blade depending on varied wind speed	CFD can capture non-uniform flow around the blade, including variations in wind speed and direction, and can account for the blade twist. FEA would give a more accurate value for the deflection as it accounts for the internal geometry and material properties of the blade

Pitch Drive Gear:

Motor Hoyer AC IE4, model HMC4-225M-2 was selected as the outsourced pitch drive motor due to its properties listed in Table 26 and its high efficiency. It requires less energy and has lower operational costs compared to IE3,2,1 motors.

Table 26: Properties of the pitch drive motor

Motor Hoyer AC IE4				
Output Power	Speed	Voltage	Frequency	Frame Size
45 kW	3000 rpm	400 V	50 Hz	225 mm

GP400 [f] was used to provide the parameters required to design the pitch drive pinion and ring gears as shown in Table 27. The forces and torque acting on the pinion and ring gears were calculated using Equations 26, 27 and 28 and are shown in Table 27.

$$T = \frac{60}{2\pi} \cdot \frac{P}{v} \quad (26)$$

$$F_t = \frac{2T}{D} \quad (27)$$

$$F_r = F_t \tan \phi \quad (28)$$

Table 27: Parameters of pinion and ring gears

	Pinion	Ring
Gear Type	External Spur	Internal Spur
Material	Low Alloy Steel, AISI 4340	Carbon Steel, AISI 1095
Number of Teeth	27	288
Pitch Circle Diameter (mm)	189	2016
Outer Diameter (mm)	200	2500
Internal Diameter (mm)	40	2000
Root Diameter (mm)	172	2030
Speed, rpm	3000	281
Power (kW)	Input- 45	Output- 4.22
Torque (Nm)	143	1528
Tangential Force, F_t (N)	1513	-1513
Radial Force, F_r (N)	551	-551
Gear Ratio	10.67	
Centre Distance (mm)	914	
Addendum (mm)	7	
Dedendum (mm)	8.75	
Pressure Angle	20	
Module (mm)	7	
Face-width (mm)	150	

The meshing of the two gears is shown in Figure 30 along with labelled parameters in Table 27.

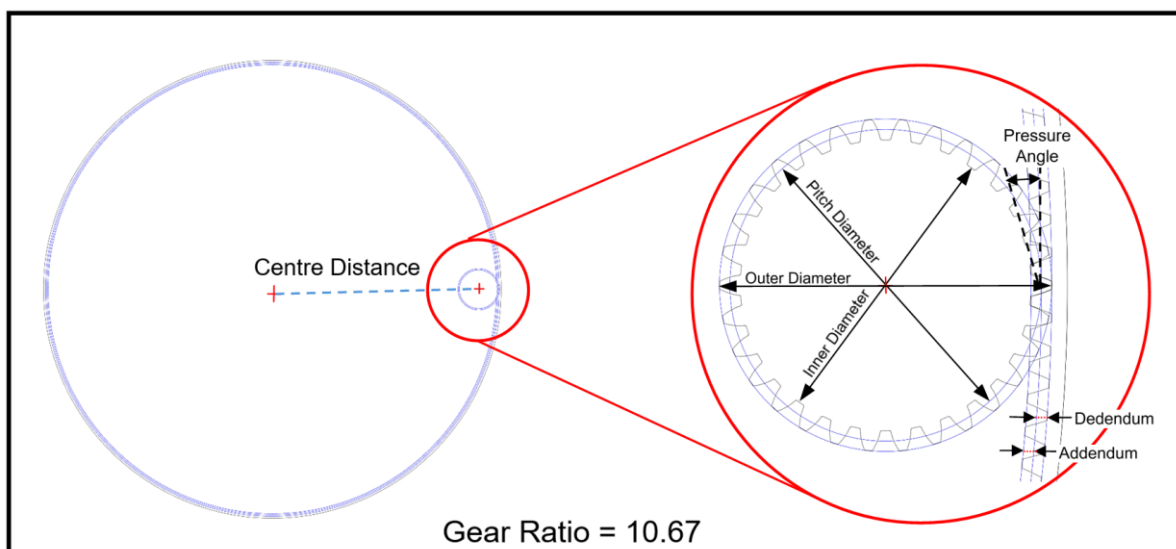


Figure 30: Gear meshing between external pinion and internal ring gears

Low Speed Shaft:

The low-speed shaft is a critical component as it transfers power from the rotating turbine to the gearbox. Calculations were necessary for this component to ensure it could withstand torsional loads, fatigue and stress between the turbine and the gearbox.

Research was conducted to identify the best material for a mechanical shaft. Granta EduPack [i] was used, due to its comprehensive materials database, to identify Stainless Steel 410 as the most suitable material, as it has a high tensile strength and good machinability. Its properties listed in Table 28.

Table 28: Properties of material (Stainless Steel 410)

Density	Young's Modulus	Yield Strength	Ultimate Tensile Strength	Shear Modulus	Fracture Toughness
7750 kg.m ⁻³	190 GPa	776 MPa	510 MPa	74 GPa	119 MPa.m ^{1/2}

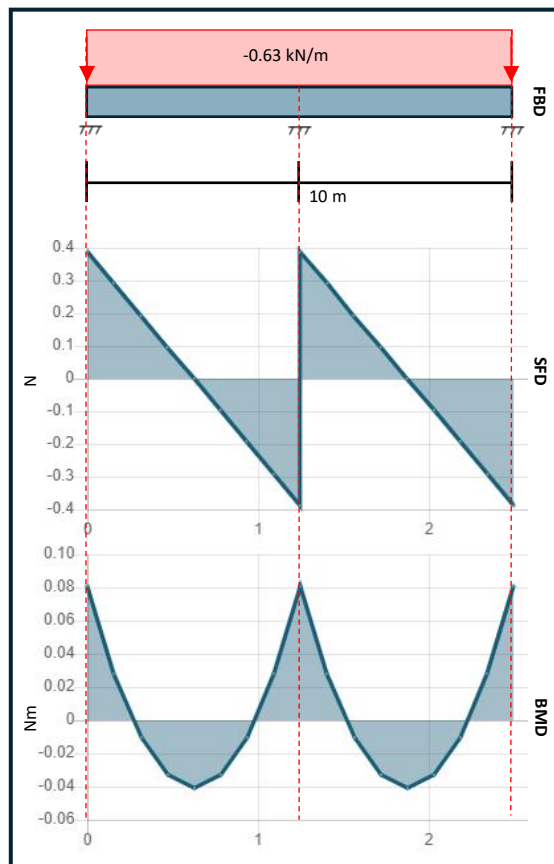


Figure 31: FBD, SFD and BMD for shaft

The low-speed shaft features two fixed points: one at the rear of the hub and another at the gearbox entrance, with an additional fixed-point bearing located at the centre of the shaft. SkyCiv [g] was used to solve for the resultant forces on the shaft which provided the bending moments and shear forces, as seen in Figure 31. Figure 31 also illustrates a free body diagram showing the resultant and reaction forces. A length of 10 m was used for the length of the shaft. The shear force and bending moment diagrams in Figure 31 shows the variation in shear force across the beam as well as the section of the beam that will be subject to maximum bending moment.

From diagrams in Figure 31:

- Max Shear Force: **0.39 kN**
- Min Shear Force: **-0.39 kN**
- Max Bending Moment: **0.04 kNm**
- Min Bending Moment: **-0.08 kNm**

The minimum shaft diameter was calculated using Equation 29.

$$d_{min} \geq \left[\frac{32f_s}{\pi S_y} \sqrt{M^2 + T^2} \right]^{\frac{1}{3}} \quad (29)$$

Table 29 shows the properties needed to work out the minimum diameter for the shaft.

Table 29: Parameters for minimum diameter of the shaft

Notation	Parameter	Value	Unit
S _y	Yield Strength	205	MPa
f _s	Safety Factor	3	-
M	Bending Moment	40.4	Nm
T	Torque	1.63 x 10 ⁶	Nm
d _{min}	Minimum Diameter	1.62	m

The deflection of the shaft is important in shaft analysis. Too much linear or torsional deflection can affect the shaft's performance and cause it to fail. Deflection was calculated by employing Equations 30 and 31, using the parameters shown in Table 30.

$$\delta = \frac{PL^3}{48EI} \quad (30) \qquad \theta = \frac{TL}{GJ} \quad (31)$$

Table 30: Parameters used to calculate linear and torsional deflection

Notation	Parameter	Value	Unit
P	Resultant Force	1575	N
T	Torque	1.63 x 10 ⁶	Nm
L	Distance Between Fixed Points	2.5	m
E	Youngs Modulus	190 x 10 ⁹	Pa
G	Shear Modulus	74 x 10 ⁹	Pa
I	Moment of Inertia	6.36 x 10 ⁻³	m ⁴
J	Polar Moment of Inertia	1.27 x 10 ⁻²	m ⁴
δ	Linear Deflection	4.2 x 10 ⁻⁷	m
θ	Torsional Deflection	0.25	deg

The critical shaft speed was calculated using Equation 32 and is shown in Table 31.

$$N_c = \frac{30}{\pi} \sqrt{\frac{g}{\delta_{max}}} \quad (32)$$

Table 31: Parameters used to calculate critical speed

Notation	Parameter	Value	Unit
g	Gravitational Field Strength	9.81	ms ⁻²
δ _{max}	Maximum Linear Deflection	4.2 x 10 ⁻⁷	m
N _c	Critical Speed	46151	rpm

2.6.3 / Finite Element Analysis

To allow for bending calculations to be carried out, the blade was simplified to a cantilever beam. This assumption does not accurately reflect the effect of the aerofoil shape, the different chord lengths and twist angles, or the internal webbed structure of the blade. Thus, FEA was implemented to generate more accurate reflections on the stresses and displacements of the blade that considers the shape and the internal features. This was carried out using Autodesk Fusion 360 [h].

Table 32: Justification of modelling simplifications.

Reason for simplifications		
The ideal model that would accurately reflect the blade, would be a model of the full 60 m length blade with the internal features included as shown in Figure 48. However, it was found that this model would not mesh or solve in the FEA software. Thus, model simplifications were required.		
Simplification	Justification	Limitation
The internal features were removed and the blade was modelled as a solid body as shown in Figure 49.	Enable us to obtain results that reflect the stresses and displacements present in the full 60 m length blade.	There will be differences in the stress distributions and stress concentrations predicted by a model of a solid blade, compared to a model of a blade with internal features. This can affect our results.
The blade model was sliced into 2 parts as shown in Figures 32 and 33. These parts included the internal webbed structures and were able to mesh and solve on Fusion 360. A simplified solid model of these 2 parts were created as shown in Figures 34 and 35. The distribution and the maximum values of stress and deflection were compared between the solid version and internal structure version of the blades.	This was used to analyse the differences between the results of the solid models vs the models with internal features. These differences can then be then taken into consideration when analysing the results from the solid model of the full length of the blade.	-

Tables 33 and 35 outline the model simplification, input boundary conditions and meshing conditions. Tables 34a, 34b, and 35 outline the results for the spliced component models and the full 60 m blade model respectively.

Table 33: Model simplifications and boundary conditions used for FEA analysis

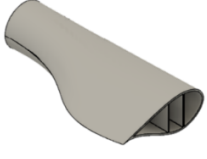

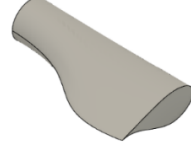

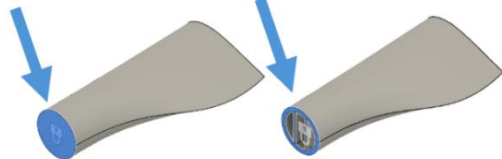
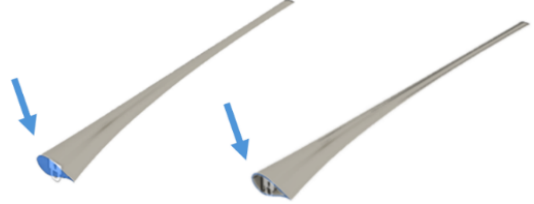
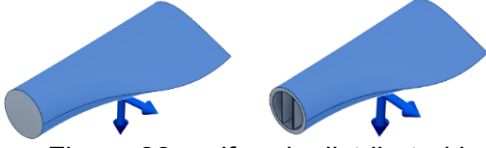
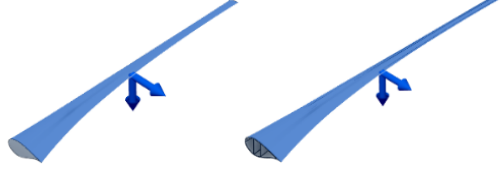
Model	
Model: Static stress analysis	Justification: Suitable for analysing the deformation and stress in the model.
 <p>Figure 32: Variation 1 - simplified CAD model of a portion of the wind turbine blade with the internal webs.</p>	 <p>Figure 33: Variation 2 - simplified CAD model of a portion of the wind turbine blade with the internal webs.</p>
Model Simplification	
 <p>Figure 34: Variation 3 - simplified CAD model of a portion of the wind turbine blade modelled as a solid component.</p>	 <p>Figure 35: Variation 4 - simplified CAD model of a portion of the wind turbine blade modelled as a solid component.</p>
Mesh Settings	
<p>Settings:</p> <ul style="list-style-type: none"> • Automeshing. • Tetrahedral solid elements. • Element size 5% - 10% of model size. • Curved mesh elements 	<p>Justification:</p> <ul style="list-style-type: none"> • Literature suggests automeshing is suitable for complex models [18]. • Used for meshing volume structures (3D solid CAD models) [18]. • Recommended by autodesk for solid elements [19]. • Recommended by autodesk for accurate representation. [19]
Boundary Conditions	
 <p>Figure 36: arrow indicating the face used to apply a fixed boundary condition to the two blade models (variations 1 & 3).</p>	 <p>Figure 37: arrow indicating the face used to apply a fixed boundary condition to the two blade models (variations 2 & 4).</p>
The faces selected in Figures 36 and 37 were fixed in the x, y, and z directions.	
 <p>Figure 38: uniformly distributed loads applied to the two blade models (variations 1 & 3).</p>	 <p>Figure 39: uniformly distributed loads applied to the two blade models (variations 2 & 4).</p>
Using values from the calculations stage, the resultant flapwise UDL of 9.77 kN/m, and the edgewise UDL of 16.22 kN/m, were applied to the model as uniformly distributed loads in the vertical and horizontal directions respectively, as shown in Figures 38 and 39.	

Table 34a: Results 1 - stress analysis of solid and internally structured blades





Results 1	
Effect of simplification on stress	
 <p>Figure 40: Autodesk Fusion360 FEA stress results for variation 3, a solid model of a section of the blade.</p>	 <p>Figure 41: Autodesk Fusion360 FEA stress results for variation 4, a solid model of a section of the blade.</p>
 <p>Figure 42: Autodesk Fusion360 FEA stress results for variation 1, a model of a section of the blade including the internal features.</p>	 <p>Figure 43: Autodesk Fusion360 FEA stress results for variation 2, a model of a section of the blade including the internal features.</p>
<p>The results from Figures 40 and 42 show that the maximum stress in variation 1 (0.124 MPa), is approximately 2.75 times greater than in variation 3 (0.045 MPa). This indicated that the solid model underestimates the stress in the blades.</p>	<p>The results from Figures 41 and 43 show that the maximum stress in variation 2 (2.098 MPa), is approximately 1.8 times greater than in variation 3 (1.144 MPa). This indicated that the solid model underestimates the stress in the blades.</p>
<p>The results from both models show that the general location of maximum stress is the same (root, centre, or tip), but the specific locations differ slightly. This is likely because the model with the internal features will distribute the stress differently.</p>	
<p>As both model results show that the solid model gives an underestimation, when analysing the stress on the full 60 m blade model, this underestimation should be taken into account. To do so, the upper value of 2.75 will be used. The maximum stress predicted by the solid 60 m blade model should be multiplied by 2.75 to estimate the likely stress if the model were to have internal features. This new value should then be used to inform the design and material selection of the blade.</p>	
<p>Figures 42 and 43 also show that the maximum stress on the blades, occurs on the outer structure rather than on the internal web structure. Based on the colour gradient, the internal web structure tends to experience a lower amount of stress. This indicates that an internal web structure is suitable to use to decrease the weight of the blade as long as the outer surface is reinforced to account for the higher stresses.</p>	

Table 34b: Results 2 - flapwise displacement analysis of solid and internally structured blades

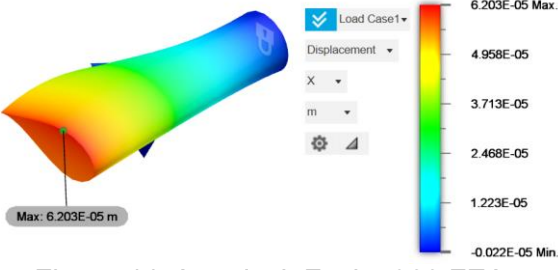
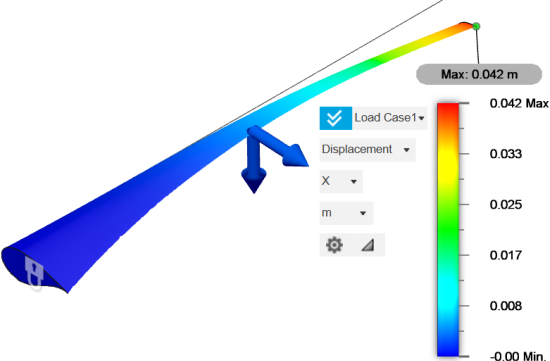
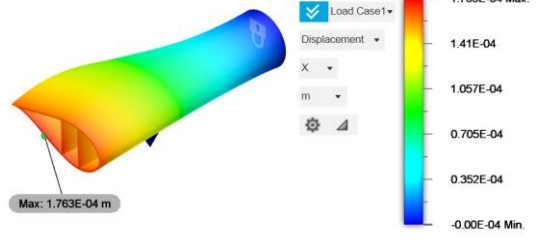
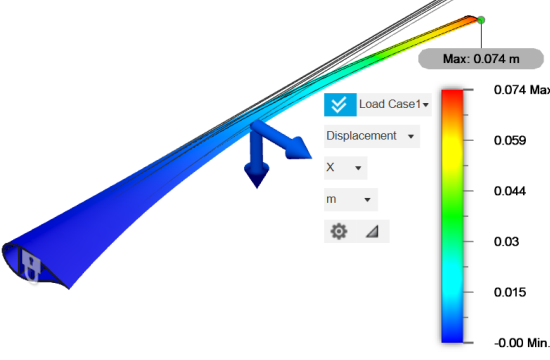
Results 2	
Effect of simplification on flapwise displacement	
 <p>Figure 44: Autodesk Fusion360 FEA displacement results for variation 3, a solid model of a section of the blade.</p>	 <p>Figure 45: Autodesk Fusion360 FEA displacement results for variation 4, a solid model of a section of the blade.</p>
 <p>Figure 46: Autodesk Fusion360 FEA displacement results for variation 1, a model of a section of the blade including the internal features.</p>	 <p>Figure 47: Autodesk Fusion360 FEA displacement results for variation 2, a model of a section of the blade including the internal features.</p>
<p>The results from Figures 44 and 46 show that the maximum flapwise displacement in variation 1 (17.63×10^{-5} m) is approximately 2.8 times larger than in version 3 (6.203×10^{-5} m). This indicates that the solid model underestimates the maximum flapwise displacement of the blades.</p>	<p>The results from Figures 45 and 47 show that the maximum flapwise displacement in variation 2 (7.4×10^{-2} m) is approximately 1.8 times larger than in version 4 (4.2×10^{-2} m). This indicates that the solid model underestimates the maximum flapwise displacement of the blades.</p>
<p>The results from both models show that the general location of maximum displacement is the same (root, centre, or tip), but the specific locations differ. This is likely because the model with the internal features will distribute the displacement differently.</p>	
<p>As both model results show that the solid model gives an underestimation, when analysing the displacement on the full 60 m blade model, this underestimation should be taken into account. To do so, the upper value of 2.8 will be used. The maximum displacement predicted by the solid 60 m blade model should be multiplied by 2.8 to estimate the likely displacement if the model were to have internal features. This new value should then be used to inform the design and material selection of the blade.</p>	

Table 35: Model simplifications and boundary conditions used for FEA analysis of the full length blade


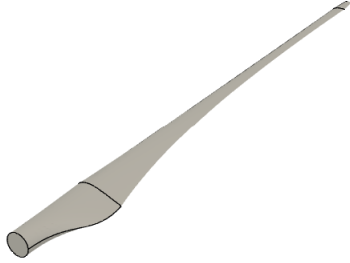

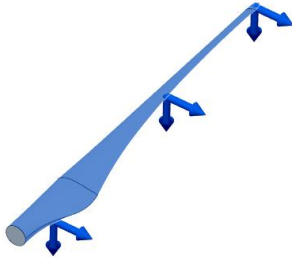
Model (Full length blade)	
Model: Static stress analysis	Justification: Suitable for analysing the deformation and stress in the model.
Original Blade Model	
	
Figure 48: CAD model of the full length of the wind turbine blade.	
Model Simplification	
	
Figure 49: Simplified solid CAD model of the full length of the wind turbine blade with the internal webs removed.	
Mesh Settings	
Settings: <ul style="list-style-type: none"> • Automeshing. • Tetrahedral solid elements. • Element size 5% - 10% of model size. • Curved mesh elements 	Justification: <ul style="list-style-type: none"> • Literature suggests automeshing is suitable for complex models [18]. • Used for meshing volume structures (3D solid CAD models) [18]. • Recommended by autodesk for solid elements [19]. • Recommended by autodesk for accurate representation [19].
Boundary Conditions	
	
Figure 50: Fixed constrained applied to one face of the CAD model. Arrow indicating the face.	Figure 51: Uniformly distributed load (UDL) applied to the blade in the flapwise direction (vertical) and edgewise direction (horizontal).
The face that connects to the blade hub was fixed in all directions as shown in Figure 50.	Using the values from the calculations stage, the resultant flapwise UDL (9.77 kN/m) and the edgewise UDL (16.22 kN/m) were applied as uniformly distributed loads, as shown in Figure 51.

Table 36: Results 3 - stress and flapwise displacement analysis on a solid model of 60 m length blade

Results 3
Full Length Blade
Stress

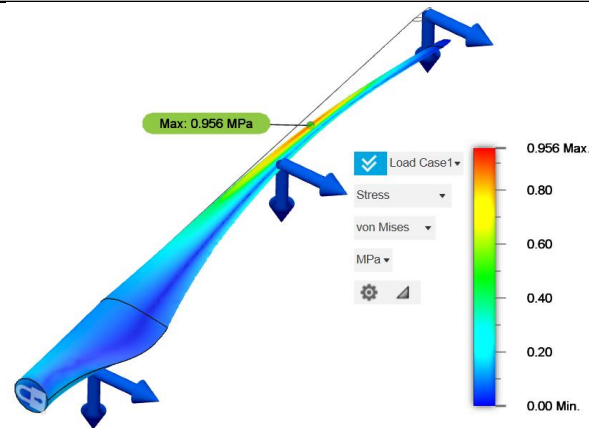


Figure 52: Autodesk Fusion360 FEA stress results for a solid model the full length of the blade.

The maximum stress predicted by the model is 0.956 MPa, as shown by Figure 52. To take into account that the solid model may not reflect the maximum stress in a model with internal structures, this value will be multiplied by 2.75 (taken from Results 1). Thus, the maximum predicted stress is 2.629 MPa.

The yield strength of the balsa wood core is 18 MPa, and the yield strength of the epoxy E-glass outer skin is 700 MPa. Following the 2/3 yield criterion, the maximum allowable yield stress is 12 MPa for the balsa wood core, and 466.67 MPa for the epoxy E-glass outer skin. The maximum predicted stress by the model is below these two values thus validating that the design is fit for its purpose.

Displacement

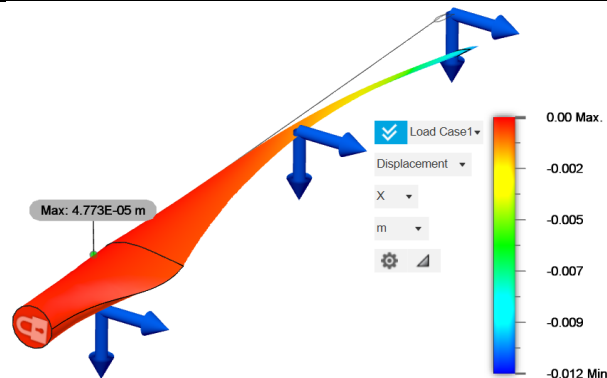


Figure 53: Autodesk Fusion360 FEA displacement results for a solid model the full length of the blade.

The maximum displacement predicted by the model is 4.773×10^{-5} m, as shown by Figure 53. To take into account that the solid model may not reflect the maximum deflection in a model with internal structures, this value will be multiplied by 2.8 (taken from Results 2). Thus, the maximum predicted flapwise displacement in the blades is 9.546×10^{-5} m.

Literature suggests that the flapwise deflection not exceed 4.5 m (30% of the clearance between the blade tip and the turbine tower) [20]. The maximum deflection predicted by the model is significantly lower than this. Thus, validating that the blade deflection is in an acceptable range and the blade design is fit for it's purpose.

2.6.3 / Failure Mode and Effects Analysis

A Failure Mode and Effects Analysis (FMEA) in Table 38 was carried out to achieve the objective in the PDS of identifying any possible failures, the causes, and ways to control these. A scale of the severity, occurrence and detection is included in Table 37 which were used to calculate the final risk priority number (RPN) to quantify which failures were the most critical.

Table 37: Scale for the severity, occurrence, and detection

Severity (SEV)	Low Impact Event	1 2 3 4 5 6 7 8 9 10	High Impact Event
Occurrence (OCC)	Low Frequency	1 2 3 4 5 6 7 8 9 10	High Frequency
Detection (DET)	Easily Detected	1 2 3 4 5 6 7 8 9 10	Impossible to Detect

Table 38: FMEA of the wind turbine components

Process Step	Potential Failure Mode	Potential Failure Effect	SEV	Potential Causes	OCC	Current Process Controls	DET	RPN (SEV x OCC x DET)	Action Recommended
What is the process step under investigation?	In what ways can the step go wrong?	What is the impact if this is not prevented or corrected?		What causes the step to go wrong?		What controls exist that either prevent or detect the failure?			What are the recommended actions for reducing the occurrence of the cause or improving detection?
Change of blade pitch	Fast rotation of blades	Failure of pitch mechanism	7	High wind speed	4	Sensors/braking systems	2	56	
Pitch bearing replacement	Bolts could break or deform	Turbine operation stopped	10	Over/under torque of bolts	1	Torque limiting devices that are colour coded	8	80	Use torque control software to track and record torque values during assembly
Seal contamination	Unclean environment	Reduced performance and increased friction	4	Debris/ dirt enters during installation	6	Inspecting seals for cleanliness	8	192	Maintain clean and controlled working environment
Installation of blades	Misalignment of blades	Blade tip rubbing	9	Human error	4	Alignment/tilt sensors	5	180	Experience and training of staff
Environmental conditions	Deflection of blades	Increased loads on hub and fatigue	10	Natural disasters (e.g. Storms)	3	Strain gauges and load sensors	2	60	Vibration monitoring system

Hub/Blade coating	Abrasion	Reduced performance	6	Coating wears off	4	Surface preparation	4	96	
Short circuits within the pitch motor	Electrical Failure in Pitch Motor	Inability to adjust blade and potential shutdown	9	Disconnected wires, overheating and excessive mechanical loading	4	Temperature and torque sensors	1	36	Use thermal imaging to detect hot spots in electrical circuits
Sensor	Sensor Failure within pitch drive	Incorrect blade pitch adjustments due to inaccurate wind speed or direction data	3	Different environmental conditions can cause damage to sensor	6	Protective coating	7	126	Protective enclosures that protect against debris
Pitch Gear teeth	High and repeated loading	Gear teeth wear and deformation	8	High torque form increased aerodynamic forces on blades	3	Monitor vibration and temperature levels to detect friction	6	144	Use high quality lubricants to reduce to reduce friction between gears

2.6.5 / Justification of Design against PDS

The final wind turbine blade design was tapered and twisted with specific aerofoils to optimise aerodynamic efficiency and structural integrity. The tapered design of the blades reduced weight towards the blade tips (objectives 1.1 and 5.2). Twisting the blades resulted in the optimal angle of attack reducing drag and enabling a high lift coefficient of 1.2 without the risk of stalling (objective 2.1).

The blade and turbine hub design achieved a balance by being lightweight and durable (objectives 5.1 and 5.2) by using high-strength, weather-resistant materials with high ductility and elastic modulus, reducing the risk of fatigue and failure. The design of the pitch drive system, low speed shaft and turbine hub prioritised reliability, performance, and ease of maintenance (objectives 3 and 4). The pitch drive system was incorporated for optimal blade angle adjustment for efficient energy capture across varying wind conditions, maintaining consistent blade speed of 9.5 rpm (objective 3.1).

Computer modelling tests, including CFD and FEA, were used to validate the performance criteria outlined in the PDS across various wind speeds (objectives 2 and 3). Sustainable practices were integrated by maximising the use of recyclable materials and considerations for decommissioning (objective 5.4 and 5.5). Overall, the final design meets the criteria outlined in the PDS of efficient energy extraction, longevity, and environmental sustainability.

2.6.6 / Limitations and Mitigations

The components of a wind turbine such as the blades, hub and low speed shaft, play crucial roles in the turbine's operation and efficiency. Table 39 shows the limitations and potential mitigation strategies for each component:

Table 39: Limitations and mitigations for different components of a wind turbine

	Limitation	Mitigation
Blade Aerodynamic Performance	The curvature of the blades can lead to complex flow patterns, including separation and turbulence, which may reduce efficiency.	Using computational fluid dynamics simulations and wind tunnel testing, curved blades can be optimised to improve aerodynamic performance and minimise negative effects.
Blade Structural Stress	The curvature of the blades can introduce additional stresses and strains, particularly under variable wind conditions common in offshore environments. This can affect the durability and lifespan of the blades.	Developing and using materials that can withstand the additional stresses induced by the curved shape can help mitigate structural issues.
Blade Manufacturing Complexity	Curved blades can be more challenging to manufacture than straight blades. The complexity of the shape can increase production time and costs.	Advances in manufacturing technologies, such as automated fibre placement and 3D printing, can reduce the complexity and cost of producing curved blades.
Hub Mechanical Stress	The hub must withstand mechanical forces, which can lead to stress fractures or mechanical failure.	Using stronger, yet lighter materials can reduce weight and improve resistance to mechanical stresses.
Hub Weight	The weight of the hub can contribute to overall nacelle weight, affecting structural support and installation costs.	Enhancing the hub design for easier access and maintenance can help in reducing downtime and maintenance costs.
Low Speed Shaft Torque Fluctuations	The low speed shaft experiences high torque fluctuations which can cause wear and fatigue.	Designing shafts with robust materials that can handle torque fluctuations better.
Low Speed Shaft Alignment Issues	Misalignment with other drivetrain components can lead to increased wear and reduced efficiency.	Ensuring precise alignment during installation and using advanced bearings can mitigate alignment issues.
Maintenance Challenges	Certain components are harder to access which makes regular maintenance difficult and costly.	Improving design for easier access as well as installing sensors can help in reducing downtime and maintenance costs.

By addressing these limitations with targeted mitigations, the performance and longevity of wind turbines can be significantly improved, contributing to more reliable and efficient renewable energy production.

2.7 / MATERIALS SELECTION: MANUFACTURED PARTS

2.7.1 / General Functional Requirements

Given the marine environment, all materials should exhibit good saltwater durability to maintain its structural integrity and increase its lifespan. To align the project with the UN SDGs, where possible the primary production energy usage, water usage, and CO2 footprint should be minimised for the materials, and recycling and downcycling should be considered.

2.7.2 / Blade Core

Functional Requirements

Table 40 below outlines the functional requirements for the blade core material to ensure it does not fail under operational conditions.

Table 40: Functional requirements for the blade core material.

Requirement	Reason
Low density	<ul style="list-style-type: none">To reduce load on turbine structure and foundations.To improve the blade's response times to changing wind conditions and thus improve energy capture efficiency.
High strength	<ul style="list-style-type: none">To withstand the bending, torsional, and compressive forces without buckling or deformation.
Fatigue resistant	<ul style="list-style-type: none">To withstand the cyclic loading conditions.

Typical Materials

Balsa wood and Polyethylene terephthalate (PET) foam [i].

Initial Screening

Figure 54 shows the parameters used for the initial screening, and the final 2 selections.

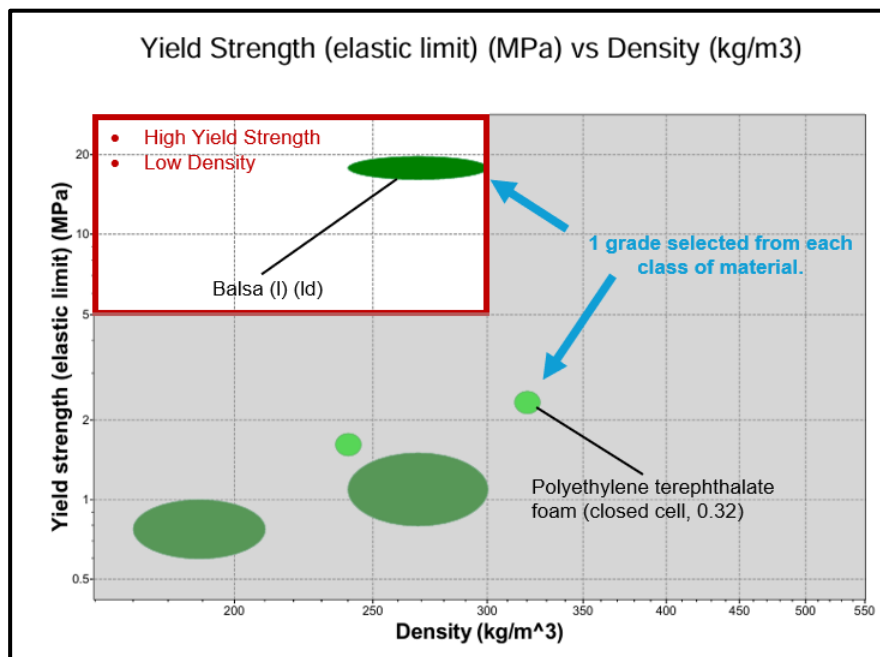


Figure 54: Yield strength vs density for balsa wood and PET foam [i]

Comparison

Table 41 and 42 below display the material properties, environmental impact, and end-of-life options for balsa wood and PET foam.

Table 41: Material properties for balsa wood and PET foam [i]

Material	Cost (GBP/kg)	Density (kg/m ³)	Specific stiffness (MN.m/kg)	Yield strength (MPa)	Fatigue Strength at 10 ⁷ cycles (MPa)	Flexural strength (MPa)
Balsa wood, longitudinal, low density	7.19	270	30	18	9.9	33
PET foam, closed cell (0.32)	8.86	315	0.52	2.15	1.8	0.61

Table 42: Environmental impact and end-of-life options for balsa wood and PET foam [i]

Material	Embodied energy, primary production (typical grade) (MJ/kg)	CO2 footprint, primary production (typical grade) (kg/kg)	Water usage, primary production (l/kg)	Recycle	Downcycle
Balsa wood, longitudinal, low density	71.6	0.373	700	No	Yes
PET foam, closed cell (0.32)	88.5	5.05	399	No	Yes

Selected Material & Justification

Table 43 below shows the chosen material for the blade core and the justification for the selection.

Table 43: Material selection & justification for the blade core material

Material	Justification
Balsa wood, longitudinal, low density	<ul style="list-style-type: none"> • Superior mechanical properties. • Lower cost. • While the primary production of balsa wood uses more water, it has lower energy usages and CO2 footprint.

2.7.3 / Blade Outer Skin & Nose Cone

Functional Requirements (blade outer skin)

Table 44 below outlines the functional requirements for the blade outer skin material to ensure it does not fail under operational conditions.

Table 44: Functional requirements for the blade outer skin

Requirement	Reason
Low density	<ul style="list-style-type: none"> To reduce load on turbine structure and foundations. To improve the blade's response times to changing wind conditions and thus improve energy capture efficiency.
High stiffness and strength	<ul style="list-style-type: none"> To withstand dynamic wind loads, including gusts, storms, and extreme weather events, without excessive deflection or deformation.
Fatigue resistant	<ul style="list-style-type: none"> To withstand the cyclic loading conditions.

Functional Requirements (nose cone)

Table 45 below outlines the functional requirements for the nose cone material to ensure it does not fail under operational conditions.

Table 45: Functional requirements for the nose cone

Requirement	Reason
Low density	<ul style="list-style-type: none"> To reduce load on turbine structure and foundations and improve ease of installation.
Corrosion and wear resistance	<ul style="list-style-type: none"> To provide environmental protection for the components within the nacelle.

Typical Materials (blade outer skin & nose cone)

Carbon fibre reinforced polymer (CFRP) composites, and glass fibre reinforced polymer (GFRP) composites. [i]

Initial Screening (blade outer skin & nose cone)

Figure 55 shows the parameters used for initial screening and the final 2 selections.

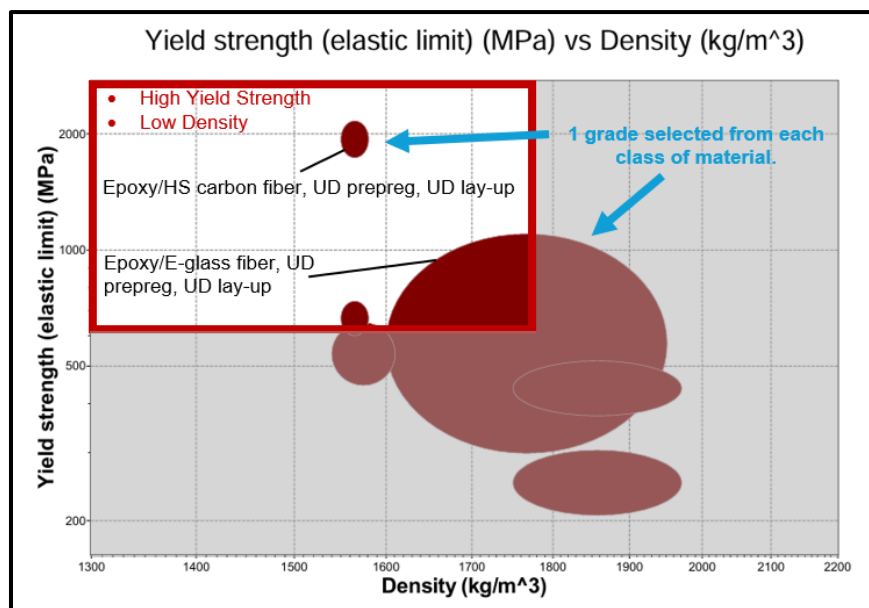


Figure 55: Yield strength vs density for Epoxy E-glass fibre composites and Epoxy carbon fibre composites [i].

Comparison (blade outer skin & nose cone)

Table 46 and 47 below display the material properties, environmental impact, and end-of-life options for Epoxy E-glass fibre composites and Epoxy carbon fibre composites.

Table 46: Material properties for a grade of CFRP composite and GFRP composite [i]

Material	Cost (GBP/kg)	Density (kg/m ³)	Specific stiffness (MN.m/kg)	Yield strength (MPa)	Fatigue Strength at 10 ⁷ cycles (MPa)	Vickers Hardness (HV)	Saltwater durability
Epoxy/E-glass fibre, UD prepreg, UD lay-up	24.15	1,775	22.75	700	440	46	Excellent
Epoxy/HS carbon fibre UD prepreg, UD lay-up	33	1,565	90.5	1,955	1,184	16	Excellent

Table 47: Environmental impact and end-of-life options for CFRP composite and GFRP composite [i]

Material	Embodied energy, primary production (typical grade) (MJ/kg)	CO2 footprint, primary production (typical grade) (kg/kg)	Water usage, primary production (l/kg)	Recycle	Downcycle
Epoxy/E-glass fibre, UD prepreg, UD lay-up	118	7.28	162	No	Yes
Epoxy/HS carbon fibre UD prepreg, UD lay-up	729	51	1,410	No	Yes

Table 47 shows that the primary production of CFRP requires 6 times more energy usage, 7 times more water usage and releases 9 times more CO2 than GFRP. Thus, primary production of CFRP has a higher environmental impact. This affects what type of downcycling method is appropriate. Literature suggests that GFRP should be downcycled using low impact mechanical recycling methods e.g grinding and co-processing. For CFRP, because the primary production is energy-intensive, with much higher costs and carbon footprint, the carbon fibres are considered high value [21]. The reuse of CF can offset the carbon footprint associated with its production [21]. Thus, for CFRP, chemical processing such as solvolysis and thermal processing such as pyrolysis should be used to reclaim the higher value fibres [21] [22]. Table 48 below assesses these downcycling methods.

Table 48: Downcycling options for CFRP composite and GFRP composite [22]

Reprocessing method	Process	TRL GFRP	TRL CFRP	Cost	Scale	Environmental Impact	End product / Uses
Mechanical	Grinding	9	6	Low	Large	Low	GFRP powder for filler or reprocessing
	Cement kiln co-processing	9	N/A	Low	Large	Low	Energy recovery and cement clinker
Chemical	Solvolysis	5	6	High	Small	High	Good quality GF (70%). High quality CF (90%). Matrix material
Thermal	Pyrolysis	5	9	High	Small	High	Low quality GF. High quality CF (90%). Oils from resins.

Selected Material & Justification (blade outer skin & nose cone)

Table 49 below shows the chosen material for the blade outer skin and nose cone and the justification for the selection.

Table 49: Material selection & justification for the blade outer skin & nose cone material.

Material	Justification
Epoxy/E-glass fibre, UD prepreg, UD lay-up	<ul style="list-style-type: none"> • CFRP has a significantly higher environmental impact. • According to the FEA results, the maximum predicted yield stress is 2.629 MPa which is lower than 700 MPa. Thus, GFRP can be used whilst meeting a safety criterion of > 2/3 the yield stress. • Mechanical reprocessing has a higher Technology Readiness Level (TRL), higher scalability, lower environmental impact, and lower cost.

Components

Hub, Shaft, Ring Gear, Pinion Gear, Pinion Coupling, Bearing, Bearing housing, Bolts.

Functional Requirements

Table 50 below outlines the functional requirements for the material for metallic components to ensure it does not fail under operational conditions.

Table 50: Functional requirements for the metallic components.

Material	Requirement	Reason
Hub	Low density	<ul style="list-style-type: none"> To reduce load on turbine structure and foundations and improve ease of installation.
	Wear and fatigue resistant	<ul style="list-style-type: none"> To withstand the dynamic loading conditions that result from the rotating blades and environment.
Shaft	High stiffness and strength	<ul style="list-style-type: none"> To withstand dynamic wind loads, including gusts, storms, and extreme weather events, without excessive deflection or deformation.
	Wear and fatigue resistant	<ul style="list-style-type: none"> To withstand the cyclic loading conditions, friction, and contact stresses.
Ring Gear	High strength and toughness	<ul style="list-style-type: none"> To withstand dynamic, impact, bending and contact loads.
Pinion Gear	Wear and fatigue resistant	<ul style="list-style-type: none"> To withstand the cyclic loading conditions, friction, and contact stresses.
Pinion Coupling	Low thermal expansion	<ul style="list-style-type: none"> To reduce changes in dimensions resulting from fluctuations in temperature. This maintains the precision of the teeth thus reducing noise.
	High thermal conductivity	<ul style="list-style-type: none"> To dissipate heat generated from friction.
Bearing Housing	High strength	<ul style="list-style-type: none"> To withstand the operational loads e.g axial and radial loads from the rotor blades.
	Wear and fatigue resistance	<ul style="list-style-type: none"> To withstand the cyclic loading conditions, friction, and contact stresses.
	Low thermal expansion	<ul style="list-style-type: none"> To reduce changes in dimensions resulting from fluctuations in temperature. This maintains the precision of the teeth thus reducing noise.
Custom Bolts	High strength and toughness	<ul style="list-style-type: none"> To withstand the operational loads without failing.
	Wear and fatigue resistance	<ul style="list-style-type: none"> To withstand the cyclic loading conditions, friction, and contact stresses.

Typical Materials

Aluminium, low alloy steels, carbon steels, stainless steels.

Initial Screening

Figure 56 shows the parameters used for initial screening and the final 4 selections.

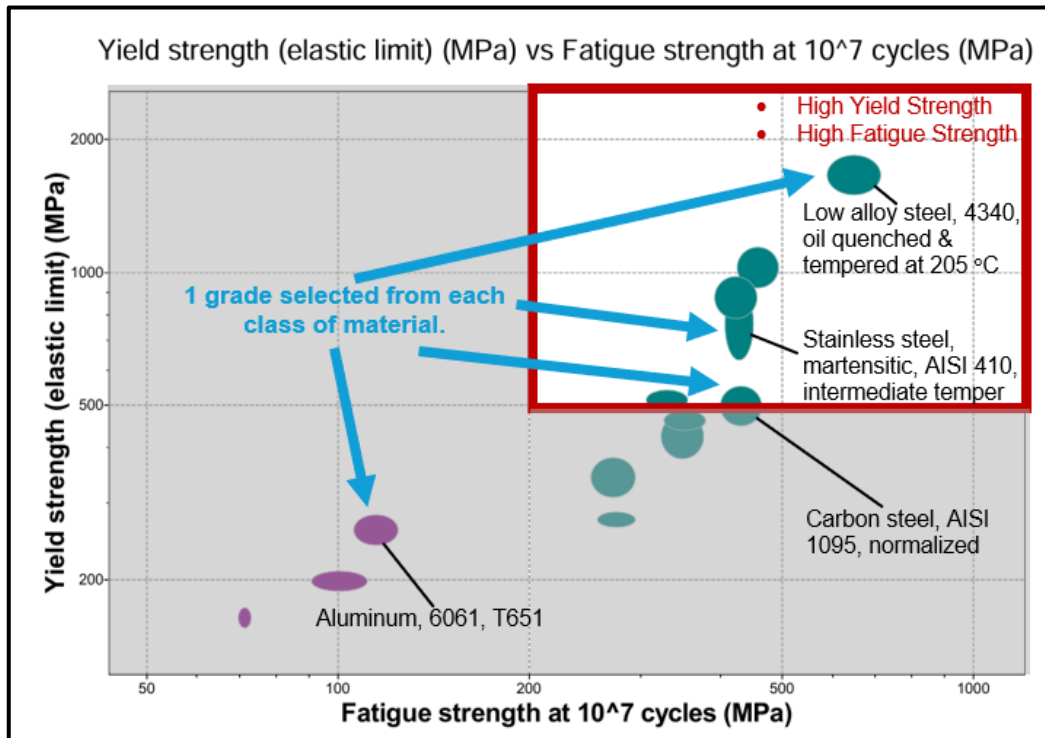


Figure 56: Yield strength vs fatigue strength for different grades of aluminium, carbon steel, low alloy steel, and stainless steel [i].

Comparison

Table 51 and 52 below display the material properties, environmental impact, and end-of-life options for the selected metals.

Table 51: Material properties for different metals [i].

Material	Cost (GBP/kg)	Density (kg/m ³)	Yield strength (MPa)	Fatigue Strength at 10 ⁷ cycles (MPa)	Vickers Hardness (HV)	Thermal conductivity (W/m.°C)	Saltwater durability
Low alloy steel, AISI 4340, oil quenched, tempered at 205 °C	1.43	7,850	1,680	651	520	36	Limited

Carbon steel, AISI 1095, oil quenched, tempered at 315 °C	1	7,850	813	504	380	49	Limited
Stainless Steel AISI 410, intermediate temper	1.67	7,750	776	428	260	25	Excellent
Aluminium, 6061, T651	2.90	2,710	261	115	104	167	Acceptable

Table 52: Environmental impact and end-of-life options for different metals [a].

Material	Embodied energy primary production (MJ/kg)	CO2 footprint, primary production (kg/kg)	Water usage, primary production (l/kg)	Recycle	Downcycle
Low alloy steel AISI 4340 oil quenched, tempered at 205 °C	16.25	1.13	53.45	Yes	Yes
Carbon steel, AISI 1095 oil quenched, tempered at 315 °C	16.25	1.13	45.05	Yes	Yes
Stainless Steel AISI 410 intermediate temper	24.65	2.43	100	Yes	Yes
Aluminium, 6061, T651	109	8.03	1,190	Yes	Yes

Material Selection & Justification

Table 53 below shows the chosen material for the relevant components and the justification for the selection.

Table 53: Material selection & justification for the metallic components.

Components	Material	Justification
Hub Shaft Bearing housing Custom bolts	Stainless Steel AISI 410, intermediate temper	<ul style="list-style-type: none"> ▪ Lower density. ▪ Good mechanical performance. ▪ Smooth surface finish for shaft, bearing and bearing housing. ▪ Good durability in saltwater for components at higher risk of exposure. ▪ Lower environmental impact compared to aluminium and can be recycled and downcycled.
Pinion gear	Low alloy steel, AISI 4340, oil quenched & tempered at 205 °C.	<ul style="list-style-type: none"> ▪ Superior mechanical performance is necessary for the pinion as it will have a higher amount of contact than the ring gear. ▪ Good thermal conductivity for heat dissipation. ▪ Main limitation is the saltwater durability, however electroplating and effective sealing can be used to mitigate this. ▪ Lower environmental impact compared to stainless steel and aluminium and can be recycled and downcycled.
Ring gear Pinion coupling	Carbon steel, AISI 1095, oil quenched & tempered at 315 °C.	<ul style="list-style-type: none"> ▪ A lower fatigue strength and hardness is acceptable for the ring gear because it will not experience as much contact. ▪ Good thermal conductivity for heat dissipation. ▪ Cheaper material is necessary for the ring gear due to its significantly larger size. ▪ Main limitation is the saltwater durability, however electroplating and effective sealing can be used to mitigate this. ▪ Lower environmental impact compared to stainless steel and aluminium and can be recycled and downcycled.

Figure 57 shows a flow chart displaying a full life cycle analysis of the components of the wind turbines.

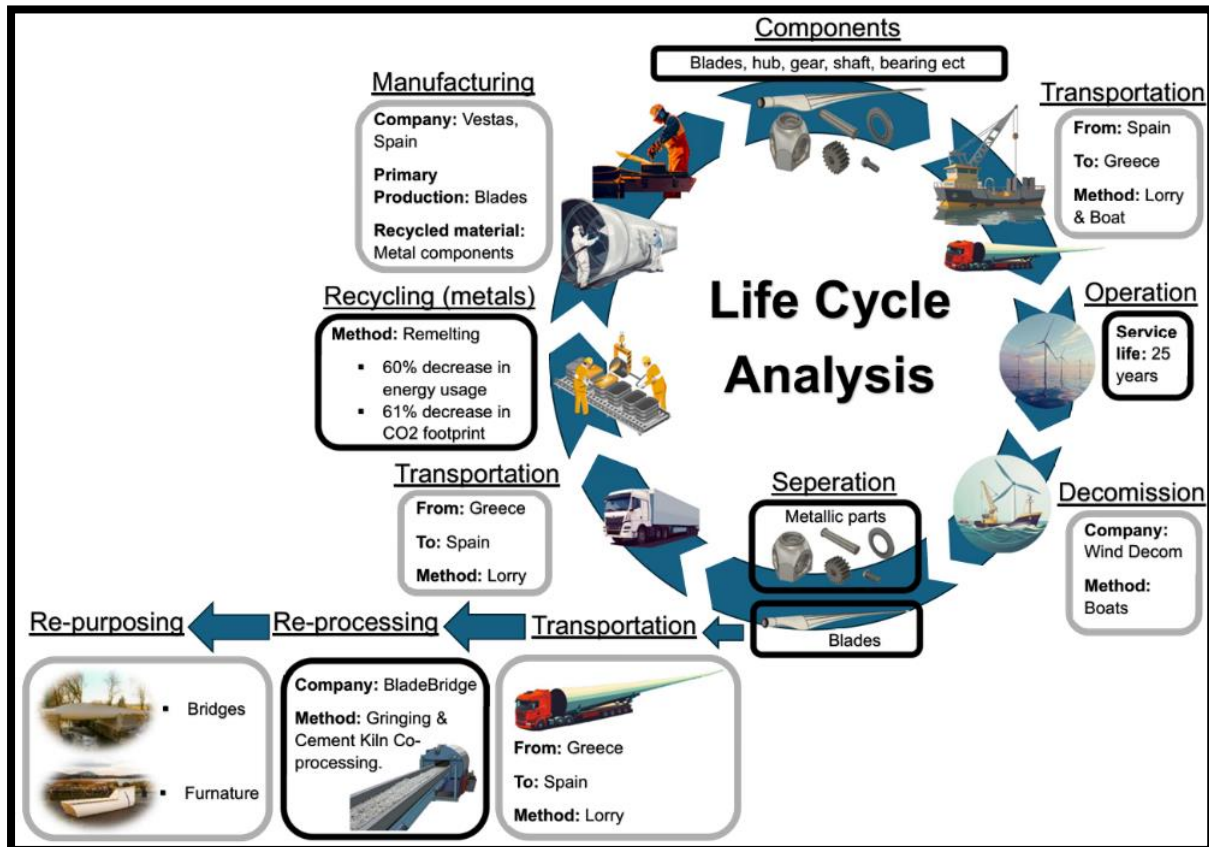


Figure 57: Life cycle analysis flow chart for different components in an offshore horizontal axis wind turbine

The components will be manufactured by Vestas, in their manufacturing facilities in Spain. This facility was selected as it is relatively close to Port Alicante Oran in Spain, thus minimising the amount of road transportation required. It was necessary to reduce road transportation due to the large size of the components, and high weight, which would make road transportation more difficult and costly. Additionally, from the port, the components can be transported directly to the location of the energy island via boat only. This minimises the frequency with which the components will be moved onto different transportation vehicles, thus minimising difficulty in the total transportation process.

The end-of-life options were researched, and it was decided that the metal components will be recycled, and the blades will be downcycled and repropesed. This allows us to avoid landfill tax and align the project with the UN SDG 12 - responsible consumption and production, and the European Commission Waste Framework Directive (2008/98/EC). This also helps contribute towards a circular economy.

2.7.6 / Life Cycle Impact Assessment

For the Life cycle impact assessment, it was assumed that manufacturing would be carried out by the company Vestas, in their facilities in Spain. The distance from the manufacturing facility to the location of the energy island was estimated. These values were inputted into Granta EduPack to obtain the results. Table 54 below shows the estimated distances and mode of transportation.

Table 54: Transportation distance and method for the wind turbine components

From	To	Distance	Method
Vestas Manufacturing Spain SL	Port Alicante Oran, Spain	350 km	Lorry
Port Alicante Oran, Spain	Offshore energy island	2,000 km	Boat

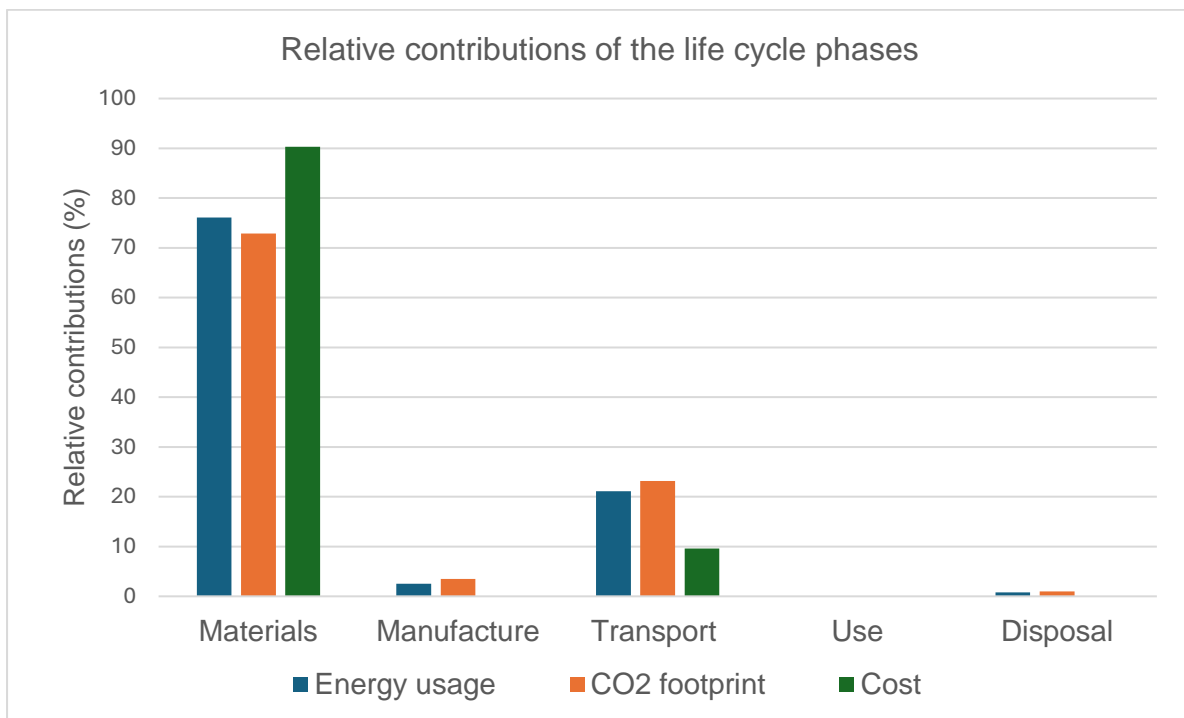


Figure 58: Relative contributions of the life cycle phases taken from Ansys Granta EduPack [i]

Figure 58 above shows that a significant amount of CO2 emissions and energy usage occurred during the primary production stages. Thus, during the materials selection stage, it was important to select materials that limited the environmental impact. This also helped to reduce carbon tax. To minimise impacts during transportation, lorry and boat transportation was selected over aircraft transportation both due to weight restrictions, and to limit the CO2 emissions.

2.8 / BILLS OF MATERIALS

The bills of materials are listed in Table 55.

Table 55: Bills of Materials

Component	Qty	Part Number	Material/Description	Cost
Blades	3	Custom	Epoxy E Glass Fiber UD prepreg, UD lay-up + Balsa Wood	£6,070,948
Low Speed Shaft (main)	1	Custom	Stainless Steel AISI 410, intermediate temper	£181,472
Turbine Hub	1	Custom	Stainless Steel AISI 410, intermediate temper	£192276
Nose Cone	1	Custom	Stainless Steel AISI 410, intermediate temper	£46814
M80 Barrel Nuts	90	Custom	Stainless Steel AISI 410, intermediate temper	£1084.86
M80 400mm Bolts	180	Custom	Stainless Steel AISI 410, intermediate temper	£9720
M80 110mm Bolts	90	Custom	Stainless Steel AISI 410, intermediate temper	£1870
M80 Locking Nuts	180	Bolts.co.uk FNMCS80	High-Strength Class 10 Steel	£8,532
M100 Locking Nuts	5	Custom	Stainless Steel AISI 410, intermediate temper	£27.95
M100 400mm Bolts	5	McMaster 91290A640	Black-Oxide Class 12.9 Alloy Steel	£153
Bearing Housing	3	Custom	Stainless Steel AISI 410, intermediate temper	£55.90
Bearing	3	NA	SKF High Endurance Slewing Bearing (Made to Order)	£300,000-£1,000,000
Ring Gear	3	Custom	Carbon steel, AISI 1095, oil quenched & tempered at 315 °C.	£2142
Pinion Gear	3	Custom	Low alloy steel, AISI 4340, oil quenched & tempered at 205 °C.	£34.32
Pinion Coupling	3	Custom	Carbon steel, AISI 1095, oil quenched & tempered at 315 °C.	£62.40
Pinion Gear Spacer	3	McMaster 93475A370	18-8 Stainless Steel	£13.13
Retaining Ring	3	McMaster 90030A123	Black-Phosphate 1060-1090 Spring Steel	£2.41
M16 260mm Coupling Bolt	3	McMaster 90447A125	High-Strength Black Class 10.9 Steel	£24.92
Pitch Driver Motor	3	Hoyer IE4 HMA4 160L-4	Aluminium	£754
M18 Motor Locking Nut	3	McMaster 90360A118	High-Strength Class 10 Steel	£19.30
M18 90mm Motor Bolts	12	McMaster 90447A138	High-Strength Black Class 10.9 Steel	£50.65

2.9 / RISK ASSESSMENT

The risk assessment was conducted by assessing and scoring the severity and likelihood of the hazard on a scale of 1 to 4, with 4 indicating the most hazardous effect and the likelihood of occurrence for the hazard as shown in Table 56. The risk factor was computed as the product of severity and likelihood, and band ratings were utilised to determine mitigating actions as shown in Table 58 which are based off the risk values in Table 57.

Table 56: Risk Assessment Scale

	Slight injuries (1 point)	Minor injuries (2 points)	Serious injuries (3 points)	Major injuries (4 points)
Very Unlikely (1 point)	1	2	3	4
Unlikely (2 points)	2	4	6	8
Likely (3 points)	3	6	9	12
Very Likely (4 points)	4	8	12	16

Table 57: Actions based on risk value

Assessed rating	1 or 2 Minimal risk	3 or 4 Low risk	6 or 8 Medium risk	9,12 or 16 High risk
Action	Remain with current measures	Evaluate current measures	Improve current measures	Stop operations and improve current measures immediately

Table 58: Risk Assessment

Hazard	Resulting Risk	Severity (out of 4)	Likelihood (out of 4)	Risk factor (severity x likelihood)	Mitigating actions
Lightning	Damage to blade surface /cracking	4	1	4	Use monitoring and early warning systems to detect lightning
	Melted blade coating	2	1	2	
Ice buildup	Added weight to blade making it unbalanced	2	3	6	Add blade heating elements to remove ice
	Projected ice pieces damaging neighbouring wind turbines	2	3	6	
Flying birds	Collision can damage surface of the blades	1	4	4	Implement habitat management practices to minimise bird attraction
	Death of animals impacts biodiversity	2	2	4	

Hail	Damage surfaces of blades	2	1	2	Protective coating used
Extreme waves	Unbalance wind turbine leading to failure of structure	3	3	9	Shut down turbines
Extreme temperature	Blades expand and contract leading to mechanical stresses	1	2	2	Install flexible couplings
Parts not properly fixed	Minor injury to crew	1	4	4	Visual and non-destructive inspections
	Major injury to crew	4	1	4	
	Blade becomes loose	3	2	6	
Working at height altitudes	Crew member falling	4	2	8	Use safety nets beneath work areas
Working around electrical devices.	Electric shock	4	2	8	Use of PPE equipment

Table 59 summarises assumptions from CFD and FEA with the respective mitigating actions taken to avoid failure of the manufacturing of the designed components.

Table 59: Assumptions and mitigation for CFD and FEA

Risk/Assumption	Mitigating Action
CFD	
Assumed flow to be steady state however this can lead to inaccuracies. Real-world conditions involve dynamic stall and flow separation, causing blade vibration and potential fatigue or failure.	Fiberglass reinforced polyester is the material used for the blade. It possesses a high damping capacity which can reduce the amplitude of the vibrations, leading to less damage.
Constant speed was assumed on CFD which is not accurate as real-world flow conditions involve fluctuations and changes in speed. This would give a misinterpretation of forces (drag and lift).	An iterative design where adjustments were made to the blade geometry, was used.
Assuming incompressible flow is valid for low speeds where density changes are negligible. However, at high speeds like at blade tips, this assumption fails, leading to inaccurate aerodynamic force predictions.	The blade design incorporates a tapered or swept-back tip to minimise the formation of shock waves and tip vortices. These features help reduce potential aerodynamic losses and structural fatigue that may result from compressibility effects at high speeds.
FEA	
Input load was assumed to be unidirectional. This can lead to stresses being underestimated which can make the design weaker than they need to be, posing a risk of failure.	Blade calculations were done to find stresses on each part of the structure.
Assumed blade was made only from GFRC in the solid model. Only using GFRC would not capture the actual behaviour of the blade.	The yield strength for the selected material is well above the predicted maximum stress of the model to account for extreme weather environments.

2.10 / FINAL DESIGN

Figure 59 illustrates an image of the final cad design with key features and components. The summary of how the technical analysis impacted the final design has been concluded in Table 60.

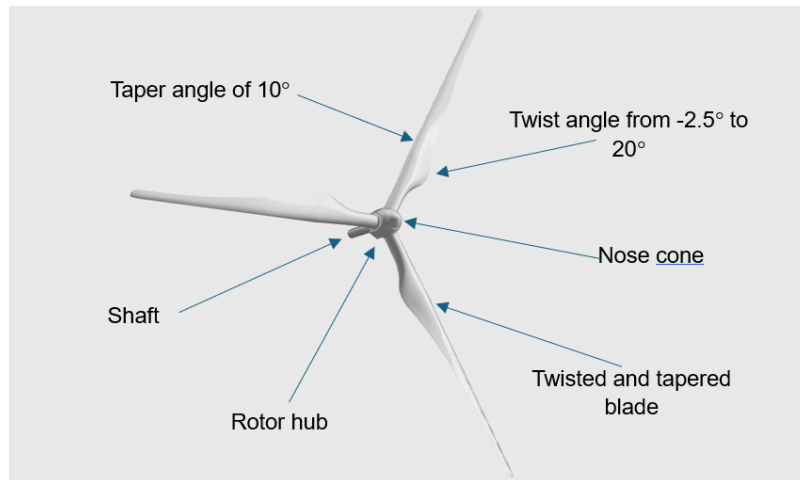


Figure 59: CAD of the final design

Table 60: Contribution of main sections to the final design

Section	Contribution to final design
2.4/ CFD	The CFD analysis offered a comprehensive comparison of the fluid flow for each of the blade variants. It was concluded that the combined twisted and tapered blade maintains the greatest lift/drag ratio (39) and torque (7.43×10^6 Nm) making it the most efficient of the three blades.
2.2/Calculations	The calculations were used to determine the optimum dimensions for the most critical components. These included the specific blade twist angles and chord lengths along the blade and to determine whether the design of the blades, main shaft and pitch drive gears would withstand the loads applied.
PDS	The PDS provided the objectives and criteria that needed to be met by the design. Emphasis on sustainability and reducing environmental impact influenced the decisions made for the final design of the components. The PDS also guided the overall technical evaluation, providing typical industry values that the calculations needed to meet.
FEA	FEA was implemented to generate more accurate estimations of the stresses and displacements of the blade that considers the shape and the internal features. From this to ensure safety and reduce the risk of failure, we ensured that the yield stress of the selected material was suitable, and we determined if the displacement was excessive.
Materials and life cycle analysis	Materials were selected to ensure that the components were fit for purpose and could withstand the operational stresses and deformation without failure. To align the project with the UN SDGs, the primary production energy usage and CO2 footprint were minimised. To avoid landfilling components, recycling and downcycling was maximised.
Research	The research findings heavily influenced the wind turbine's design. Opting for three blades, backed by higher performance coefficients. Blade shapes were selected for aerodynamic efficiency and adaptability, with twist and taper angles optimised via CFD simulations. Airfoil choices prioritized high lift-to-drag ratios, favouring DU and NACA series. Materials like GFRP were chosen for low deflection and structural integrity. Integrating these findings ensured an efficient, adaptable, and robust turbine design for the island..

2.11 / WIDER ENGINEERING IMPLICATIONS

Table 61 includes the PESTEL analysis carried out to assess and evaluate multiple external factors which have an impact on the business environment.

Table 61: PESTEL analysis of project.

P	Political	<ul style="list-style-type: none"> • Meet EU offshore wind capacity goal of 60GW by 2030. • Can be supported by upcoming scheme run by the RAE. • Compliant with regulatory framework Law 4964/2022. • Must be granted a licence from HEREMA.
E	Economic	<ul style="list-style-type: none"> • Custom M80 bolts bridge a gap within the manufacturing of offshore wind turbine blades, creating a market of selling custom bolts designed for wind turbines. • Increase in sustainable energy produced by Crete for Crete creates energy independence leading to cost savings and economic stability. • Excess energy can be sold, providing further income and profit. • Large scale project like the offshore energy island requires many staff members to maintain it. Therefore, more jobs are created boosting Crete's GDP.
S	Social/Health	<ul style="list-style-type: none"> • Increase in renewable energy leads to a reduction in energy pollution, this results in an improved public health. • Larger number of households have access to renewable energy. • Manufacturing processes of components prioritises the health and safety of the workers, creating a better working environment. • Large emphasis on engagement from stakeholders and local communities of Crete to assure that any concerns are addressed before the construction of the offshore energy island.
T	Technological	<ul style="list-style-type: none"> • Automation in manufacturing processes of components, results in faster, more efficient production. • Island location was chosen to allow for the possibility of scaling up and increasing the size of the island and wind turbines when further technological advancements are made. • Use of modern equipment, such as vibration analysers and thermographic cameras will improve diagnostic systems of the blades. • Advancements in material science allows for improved material selection of components, resulting in more durable components.
E	Environmental	<ul style="list-style-type: none"> • Blades will be made out of recycled materials were possible, promoting sustainability and reducing projects carbon footprint. • Project aligns with Greece's 2030 renewable energy targets – helping 50% of Greece's energy production be renewable. • Project will include a thorough waste management process to prevent sea pollution.
L	Legal	<ul style="list-style-type: none"> • Project needs to comply with Barcelona convention to prevent Mediterranean Sea pollution. • Project needs to abide by the EU Habitats Directive (92/43/EEC) to safeguard marine wildlife and habitats. • Project will Follow the Environmental Impact Assessment Directive (2014/52/EU) to address environmental impacts correctly. • Project will Adhere to UNCLOS for offshore energy island construction in proper maritime zones.

2.12 / BUSINESS PLAN

2.12.1 / Setting Up Business

Executive summary of business plan:

The following project involves manufacturing integral components for a wind turbine that will be on an offshore energy island off the shores of Crete. This initiative aims to provide a sustainable source of renewable energy, directly contributing to Crete's objective of achieving carbon neutrality by the year 2050. Among the components we will produce, our focus primarily revolves around the production of turbine blades. Widely regarded as the pivotal element of wind turbine efficiency, the design and construction of these blades are crucial to optimising energy output. In addition to the blades, our team has led the development of other critical components, including the turbine hub, nose hub, and pitch drive. The main objectives of the project were to increase the efficiency of the component designs whilst reducing the costs of manufacturing. Our strategy reflects our dedication to providing sustainable solutions that not only meet but surpass industry standards. Ultimately, our goal is to push Crete towards a cleaner and more sustainable future.

Team introduction:

Our team is comprised of a diverse group with a range of skills. Among us are Engineers who possess expertise in design and calculations, they utilised mathematical theorems to design the most optimal blade designs. Additionally, other team members excel in computer modelling software such as CFD and FEA, which are essential for modelling our components and aiding in determining the efficiency of our design, as well as predicting and mitigating failures. The combination of both sets of skills allowed us to produce multiple designs until we landed on the most efficient design, prioritising quality.

Furthermore, some team members focused on the manufacturing aspect of our components. They created thorough manufacturing and assembly routing sheets that employ the most efficient processes meeting engineering standards. We increased the number of automated processes to enhance efficiency and reduce labour costs. This helped develop a comprehensive and conscientious business plan. This plan prioritised cost reduction without compromising the efficiency and quality of our products.

In summary, our dynamic and diverse team, with its wide array of skills, enabled us to create designs that are not only efficient and durable but also set the industry standard.

Current Market, Growth & Trends

The current market for wind turbines is experiencing steady and stable growth due to a global demand for renewable energy sources. The percentage of renewable energy produced from wind turbines increased from 8.5% in 2004 to 17.0% in 2017 [23]. It is currently expected to grow from a market volume of 146 GW in 2024 to approximately 955 GW in 2029 [24]. Governments across the world are promoting renewable energy and there is a large market currently in Europe, making Crete a good location for a target audience of government bodies and independent power producers. The trends in wind turbine technology include increasing blade length, advanced composite materials that are also recyclable to create lighter and more durable turbines to withstand harsh environments.

Competitors

There are several companies shown in Table 62 that are currently dominating the wind turbine market due to their global presence and focus on research and development.

Table 62: Analysis of Wind Turbine Blade Competitors

Company	Description	Revenue	Strengths	Weaknesses
Siemens Gamesa, Spain (2017)	Manufacturing and services of onshore and offshore wind turbines	£7.8 billion	<ul style="list-style-type: none"> • First commercial recyclable wind turbine blades in 2022 • Strong global presence in over 90 countries • Diverse products of various rotor sizes 	<ul style="list-style-type: none"> • Relatively new company so less likely to have loyal customers
Vestas Wind Systems A/S, Denmark (1945)	Wind turbine manufacturing, installation, and service of onshore and offshore wind turbines	£12.3 billion	<ul style="list-style-type: none"> • Long history of high-quality turbines trusted by customers • Significant research and development • Worldwide installed wind capacity of 906 GW in over 80 countries 	
General Electric (GE) Renewable Energy, France (2015)	Specialise in wind, hydro and solar power. Grid integration and digital services	£12.3 billion	<ul style="list-style-type: none"> • 400 GW of renewable energy installed in over 80 countries • Various industries allow for cross-selling • Well-known and respected brand globally gains customer's trust 	<ul style="list-style-type: none"> • Market share challenged by specialised competitors
Goldwind, Beijing (1998)	Specialise in wind power, internet of energy and environmental protection	£5.4 billion	<ul style="list-style-type: none"> • Offer cost-competitive solutions making it more attractive to customers • Benefits from lower manufacturing costs in China 	<ul style="list-style-type: none"> • Challenges in markets outside China • Regulatory barriers

Figure 60 shows the product to market strategy outlining the stages of the initial design to the final product targeted at a specific audience.



Figure 60: Product to market strategy flowchart

2.12.3 / Manufacturing Costs

For parts that require manufacturing, possible methods of manufacturing were compared in terms of manufacturing cost, production rates, precision, and environmental impact using literature and the Granta EduPack database [i] [25] Methods that minimized cost, maximized production rates, maximized precision (for necessary components), and minimized environmental impacts, were selected to use for this project. The table below outlines the selected manufacturing processes, and associated tooling costs for the different components.

Table 63: Tooling costs for manufactured components, taken from Ansys Granta EduPack database [i].

Process	Method	Average Tooling Cost (GBP)
Blades (x3)		
Shaping	Vacuum assisted RTM	6,000
Joining	Epoxy adhesive	300
Surface Treatment	Water based epoxy coating (McMaster-Carr)	4,680
Hub		
Shaping	Hot open die forging	1,800
Shaping & Surface Finishing	Turning	1,300
Surface Treatment	Water based epoxy coating (McMaster-Carr)	240
Ring Gear		
Shaping	Hot closed die forging	2,000
Shaping	Milling (gear hobbing)	1,300
Surface Treatment	Shot peening	850
Pinion Gears		
Shaping	Hot closed die forging	1,450
Shaping	Milling (gear hobbing)	900
Surface Treatment	Shot peening	550
Low speed shaft		
Shaping	Hot closed die forging	2,000
Shaping & Surface Finishing	Turning	1,300
Bearing housing		
Shaping	Hot open die forging	1,800
Shaping & Surface Finishing	grinding	1,300
Nose cone		
Shaping	Vacuum assisted RTM	1,700
Surface Treatment	Water based epoxy coating (McMaster-Carr)	120
Pinion Coupling		
Shaping	Hot closed die forging	1,450
Shaping & Surface Finishing	Turning	800
Custom Bolts		
Shaping	Cold closed die forging	1,000
Shaping	Turning	700
Total tooling cost per turbine		33,540
Total tooling cost for 24 turbines		804,960

2.12.4 / Investments

The aim for acquiring investments is to:

- Fund the construction of a modern manufacturing facility with advanced equipment and technology.
- Fund the research and development of blade designs for continuous improvement and innovation.

Crete's government have invested 8 billion euros to deal with the energy crisis, of which 30% comes from the state budget. The island will use a portion of this funding as its main investment source. 70% of the production costs will be covered by the government's investment, while the remaining 20% will be secured through partnerships with external firms and investment agencies. In return for their investment, these external partners will receive a 2% return on profits upon the successful completion of the offshore energy island project. Investment companies that will be contacted include Brookfield Asset Management and Global Infrastructure Partners, due to their involvement in similar projects. The remaining 10% will be borrowed through an asset-based lending scheme which will be paid in installments after completing the project. The sources of funding have been simplified in Figure 61.

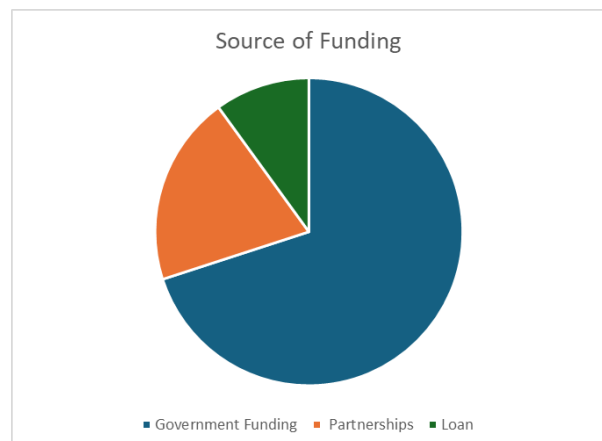


Figure 61: Pie chart illustrating the proportion of funding from each source.

2.12.5 / Rate of Return

The next section outlines the detailed breakdown of costs involved in constructing the components for the offshore energy island project. It also provides the rate of return and the profits accumulated within the first three years after the project's completion.

Table 64 below includes a summary of all costs associated with the construction of the offshore energy island, as well as the annual maintenance cost. Aside from the annual maintenance costs, the remaining cost is the initial investment made in the offshore energy island.

Table 64: Total initial cost of building offshore energy island, including yearly maintenance

Category	Cost (GBP/£)
Permitting	1,452,657
Transportation	564,000
Labour costs	1,740,400
Manufacturing costs	5,113,869
Outsourced components	229,185.84
Materials (custom)	20,946,104.40
Maintenance	695,877.76
Total	30,760,094

Figure 62 below shows the entire cost analysis and how much each category costs while developing an offshore energy island, with materials being one of the most expensive elements, as are manufacturing costs.

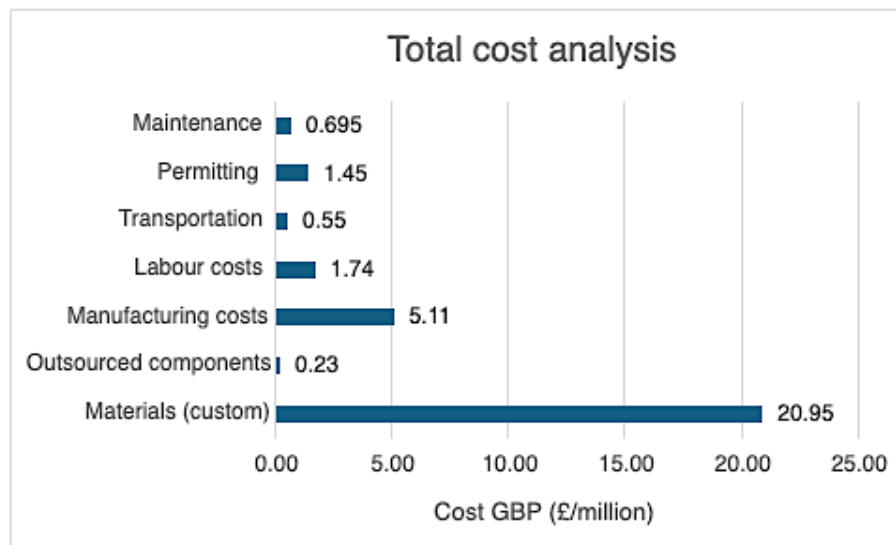


Figure 62: Total cost analysis of manufacturing offshore energy island components

Table 65 presents the investment contributions made to the offshore energy island project. As per the agreed contract, the partners will receive a 2% profit on top of their investment upon project completion. The total amounts are outlined in Table 66. Regarding the loan, repayments will be made in installments over the next 5 years. Additionally, the government funding arrangement involves providing 18% of the company's electricity output to the government for free over the next 5 years as part of a loan repayment plan. This initiative aims to promote renewable energy and enhance accessibility, aligning with Crete's sustainability objectives.

Table 65: Breakdown of Investments

Investments	Amount (GBP/£)
Government fund	21,019,751.41
Partnerships	6,005,643.23
Loan	3,002,821.63

Table 66 presents the gross and net profit made within the first three years of the island.

Table 66: Breakdown of profits

Profit (GBP)	
Gross profit	69,587,776.13
Deduction to partners (1 st year)	7397398.753
Loan payment (Next 5 years)	600,564.326
Net profit 1st year	30,829,719.05
Net profit 2nd year	68291334.37
Net profit 3rd year	68291334.37

The project's rate of return is relatively high, due to the significant upfront costs incurred predominantly in the first year. With most costs covered early on, additional revenues translate directly into profit in the coming years.

To calculate the rate of return for the first three years, equation 33 was used.

$$\text{Rate of Return (ROF)}(\%) = \frac{\text{Annual Net Profit}}{\text{Initial Investment}} \times 100 \quad (33)$$

The following Figure 63 shows the previous information graphically. The rate of return (ROF) as well as the net and gross profit of the project for the next three years. This proves the business to be financially lucrative whilst having a positive environmental impact.

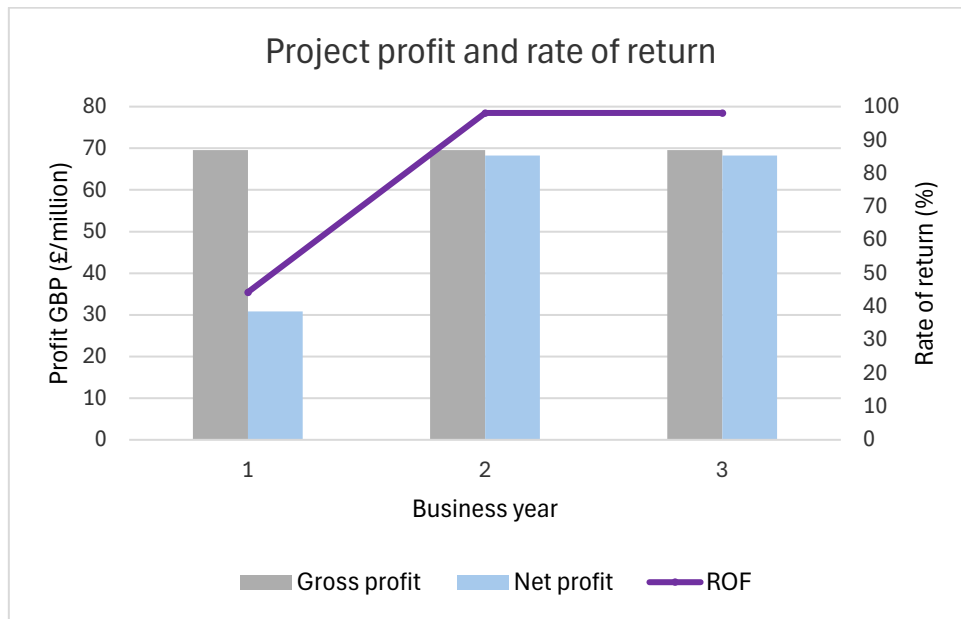


Figure 63: Bar chart of project gross and net profit – including rate of return.

Considerations and limitations:

It is noted that the rate of return and net profit values were calculated based on the profitability of the whole energy island, however, the cost breakdown in Table 64 only accounts for the components designed by Group 3. Therefore, it must be acknowledged that although cost effective practices were put into place to reduce cost and increase project rate of return, the value calculated does not directly reflect on the profitability of the project. Due to project constraints a more accruable value could not be calculated.

2.13 / ASSEMBLY ROUTE SHEET

The following section include the assembly routing sheets for the assembled components.

Table 67: Assembly routing sheet of bearing house.

Assembly name: Bearing house assembly.	Routing sheet number: 1			
	Drawing number: 1			
	Parts: Bearing housing; bearing; M80 110 mm bolts, ring gear, M80 50mm nuts.			
	Quantity: 3			
No	Operation description	Equipment/tools	Time (min)	Comments
1	Gather all components for assembly.	-	-	-
2	Inspect all components for defect or damage	-	5	Visual inspection.
3	Mount bearing into the bearing housing.	Hydraulic press.	15	Interference fit.
4	Align the ring gear with the bearing housing.	Lifting equipment (hoist)	5	Clearance fit.
5	Separately fit M80 110mm bolt into the ring gear (x30)	-	5	Clearance fit.
6	Fasten the bolt with M80 locking nuts (x30)	Pneumatic wrench + Spanner	5	-
7	Torque locking nut to 200Nm (x30)	Torque wrench + spanner	20	
8	Grease ring gear	Grease gun	2	Rheolube® 363Ax-1

Table 68: Assembly routing sheet of pinion gear and coupling

Assembly name: Pinion gear assembly.	Routing sheet number: 2			
	Drawing number: 2			
	Parts: Pinion drive coupling; Pinion gear; Pinion gear spacer; Snap ring.			
	Quantity: 3			
No	Operation description	Equipment/tools	Time (min)	Comments
1	Gather all components for assembly.	-	-	-
2	Inspect all components for defects or damage.	-	5	Visual inspection.
3	Slide the pinion gear onto the coupling.	-	1	Clearance fit.
4	Slide the pinion gear spacer	-	1	Clearance fit.
5	Expand snap ring and install it after the pinion gear spacer to hold the gear into place.	Snap ring pliers.	1	-
8	Grease pinion gear	Grease gun	2	Rheolube® 363Ax-1

Table 69: Assembly routing sheet of turbine hub assembly.

Assembly name: Turbine hub assembly.	Routing sheet number: 3			
	Drawing number: 3			
	Parts: Hub; M18 90mm motor bolts; M18 locking nuts; motor; M16 260mm pitch drive bolt; pinion gear assembly.			
	Quantity: 3			
No	Operation description	Equipment/tools	Time (min)	Comments
1	Gather all components for assembly.	-	-	-
2	Inspect all components for defects or damage.	-	10	-
3	Secure motor onto mounting bracket with M18 90mm bolts and M18 locking nuts and torque to 30Nm (x4)	Lifting equipment (hoist) + pneumatic wrench + torque wrench + spanner	5	-
4	Align bearing housing to hub and secure in place with M80 400mm bolts and M80 locking nuts (x30)	Lifting equipment (hoist) + pneumatic wrench + spanner.	15	Transition fit.
5	Torque nuts to 200Nm (x30)	Torque wrench+ spanner.	20	Clearance fit.
6	Secure Pinion assembly onto motor shaft using M16 260mm pitch drive bolt and torque to 30Nm. (x3)	Pneumatic wrench + torque wrench	5	-

Table 70: Assembly routing sheet of blade and turbine hub.

Assembly name: Blade and hub assembly.	Routing sheet number: 4			
	Drawing number: 4			
	Parts: Blade; low speed shaft; M80 250mm bolts; M80 50mm nuts; bearing housing assembly + turbine hub assembly; M80 locking nuts; M80 400mm bolts; nose; M100 400mm bolts; M100 locking nuts.			
	Quantity: 3 (1 for step 6-10)			
No	Operation description	Equipment/tools	Time	Comments
1	Gather all components for assembly.	-	-	-
2	Inspect all components for defects or damage.	-	60	-
3	Align the blade root with the mounting features on the bearing house assembly.	Crane	20	-
4	Secure the blade to the bearing housing using M80 400mm bolts and M80 barrel nuts. (x30)	Pneumatic wrench	15	Interference fit.
5	Torque the M80 400mm bolts to 200Nm. (x30)	Torque wrench.	30	Clearance fit.
6	Align hub onto the shaft.	Crane	30	Transition fit.

7	Hold shaft and hub together and secure bolts with M80 locking nuts. (x30)	Pneumatic wrench + Spanner	15	Transition fit.
8	Torque nuts to 200Nm. (x30)	Torque wrench + spanner	30	
9	Align nose onto the hub and secure in place using M100 400mm bolts and M100 locking nuts (x5)	Crane + pneumatic wrench + Spanner	25	-
10	Torque the M100 400mm bolts to 200Nm. (x5)	Torque wrench+ spanner.	5	-

2.14 / MANUFACTURING ROUTE SHEET

The following section includes the manufacturing routing sheets for all the manufactured components.

Table 71: Manufacturing routing sheet of blades.

Parts name: Blades	Routing sheet number: 1		
	Drawing number: 5		
	Quantity: 3		
No	Operation description	Machine/tools	Comments
1	General shell shape is created.	Green sand casting	Stainless steel Mould
2	Coat inside of mould with protective gel.	Airless spray system	-
3	Fiberglass is cut into blade size and fitted into mould.	CNC rotary cutting machine & automated fiber laying machine.	-
4	Route base attached to bottom of the blade for connection to hub.	Blade route attachment machine.	-
5	The carbon main spar cap is fitted in the center of only one shell.	Automated tape laying machine.	-
6	Balsa wood sheets are cut and layered into the mould.	CNC router & crane.	Workers may adjust placement.
7	Additional fiberglass sheets are fitted.	Automated fiber laying machine	-
8	Gaps filled with resin under a vacuum.	Resin infusion system.	-
9	Webs are attached.	Jigs & fixtures	-
10	2 shells are attached to each other using adhesive to form a blade.	Automated bonding machine.	-
11	Blades are demolded.	Crane	-
12	Excess material is trimmed, and surface is treated to smooth finish.	CNC router	-
13	A protective spray finish is added to the surface.	Airless spray system	-
14	Inspection/quality control.	CMM/visual inspection	-

Table 72: Manufacturing routing sheet of turbine hub.

Parts name: Turbine Hub	Routing sheet number: 2		
	Drawing number: 6		
	Quantity: 1		
No	Operation description	Machine/tools	Comments
1	General shape formed.	Forge furnace & forging press.	-

2	The surfaces and edges of hub body are milled.	CNC milling machine	-
3	Drill 80 mm diameter holes to connect blades.	CNC drilling machine	-
4	Drill 80 mm diameter holes into surface to connect nose hub.	CNC drilling machine	-
5	Surface is treated with epoxy.	Airless spray system	Epoxy adhesive DP420.
6	Inspection/quality control	5-axis CMM.	-

Table 73: Manufacturing routing sheet of turbine nose.

Part name: Turbine nose	Routing sheet number: 3		
	Drawing number: 6		
	Quantity: 1		
No	Operation description	Machine/tools	Comments
1	General shape is formed.	Vacuum assisted RTM	-
2	Drill 80 mm diameter holes to create connection with turbine hub.	CNC drilling machine	-
3	Surface of nose is sanded and polished	Handheld orbiting hander & polishing machine	-
4	Surface is painted and coated with protective coating	Airless spray system	-
5	Inspection/quality control.	5-axis coordinate-measuring machine (CMM)	-

Table 74: Manufacturing routing sheet of main shaft.

Part name: main shaft	Routing sheet number: 4		
	Drawing number: 6		
	Quantity: 1		
No	Operation description	Machine/tools	Comments
1	The general shape of shaft is forged.	Forge furnace & forging press.	-
2	Excess material is removed to achieve tight tolerances.	CNC turning machine	-
3	Material is tempered.	Tempering furnace.	-
4	Surface is coated using zinc plating.	Zinc plating tanks.	-
5	Inspection/quality control.	Control measuring machine. (CMM)	-

Table 75: Manufacturing routing sheet of bolts.

Part name: M80 bolts 400/110mm.	Routing sheet number: 5		
	Drawing number: 7		

Quantity: 180			
No	Operation description	Machine/tools	Comments
1	General shape is formed.	Forge furnace & forging press.	-
2	Head of bolt formed.	Cold heading machine.	-
3	Threads are formed along the length of the bolt.	Thread rolling machine.	-
4	Bolt undergoes heat treatment.	Quenching tank.	-
5	Surface of bolt is coated.	Zinc plating tanks.	-
6	Inspection/quality control.	Visual inspection/Rockwell test.	Rockwell HRC.

Table 76: Manufacturing routing sheet of bearing housing.

Part name: bearing Housing	Routing sheet number: 6		
	Drawing number: 8		
	Quantity: 1		
No	Operation description	Machine/tools	Comments
1	General shape is formed.	Forge furnace and forge press.	-
2	Drill 80 mm holes 90 times on the surface of the bearing housing (reference engineering drawing x)	CNC drilling machine.	-
3	General shape is machined (turning)	CNC turning machine	-
4	Inspection/quality control	Control measuring machine (CMM)	-

Table 77: Manufacturing routing sheet of ring gear

Part name: Ring gear	Routing sheet number: 7		
	Drawing number: 9		
	Quantity: 1		
No	Operation description	Machine/tools	Comments
1	Initial shape is formed	Blanking workpiece.	-
2	Internal teeth are machined.	CNC milling machine.	-
3	External teeth are broached on external circumference of the gear.	Broaching machine	-

4	Gear is deburred removing any burrs.	CNC Gear chamfering machine.	-
5	Inspection/quality control.	Control measuring machine (CMM)	-

Table 78: Manufacturing routing sheet of pinion gear.

Part name: pinion gear	Routing sheet number: 8		
	Drawing number: 10		
	Quantity: 1		
No	Operation description	Machine/tools	Comments
1	The initial shape of gear is formed.	Blanking workpiece.	-
2	Internal teeth are machined.	CNC milling machine.	-
3	The gear surface is polished.	Orbital polishers.	-
4	Inspection/quality control.	Control measuring machine (CMM)	-

Table 79: Manufacturing routing sheet of pinion coupling.

Part name: Pinion coupling	Routing sheet number: 9		
	Drawing number: 11		
	Quantity: 1		
No	Operation description	Machine/tools	Comments
1	Initial shape is formed.	Forge furnace and forge press.	-
2	Further machining is done to remove excess material and perfect cylindrical shape.	CNC turning	CNC milling can also be used – however it'll provide less accurate dimensions.
3	Component undergoes heat treatment.	Quenching tank, tempering furnace.	-
4	Teeth are cut into the coupling.	CNC milling	-
5	Coupling undergoes surface finishing.	CNC grinding tool.	BS EN ISO 1302 standard.
6	Inspection/quality control.	Visual inspection/ultrasonic testing (UT)	-

Table 80: Manufacturing routing sheet of barrel nut.

Part name: Barrel nut	Routing sheet number: 10		
	Drawing number: 12		
	Quantity: 5		
No	Operation description	Machine/tools	Comments
1	Initial shape is formed.	Band saw machine	-

2	Further machining is done to shape the nut.	CNC turning machine.	-
3	Drill 80mm hole along the length of barrel nut.	CNC drilling machine.	-
4	The hole is threaded.	Tapping machine.	M80x6mm
5	Barrel nut undergoes surface finishing to remove excess material and sharp edges.	Automated Deburring equipment.	-
6	Inspection/quality control.	Visual inspection.	-

2.15 / OPERATIONS LIST

The following section includes the operation lists for all the manufactured components.

Table 81: Operations list for the turbine blades

Part Name: Blade		List Number: 1/10					
Date: 12/04/2024		Drawing Number: 1					
		Quantity: 3					
		Planner: Sundus					
Op No	Description	Machine Tool	Tool	Cutting Speed (m/min)	Feed Rate (mm/rev)	Set Up & Op. Time (min)	Notes
1	Balsa wood panels cut into shape	CNC Router	Router Bit	200	0.2	120	Use dust collection system and use coolant
2	E-glass fibre cut into shape	Waterjet Cutter	Waterjet Nozzle	12	-	60	
3	Layup of balsa wood and E-glass fibre	Layup Table	-	-	-	180	Manual process needs proper alignment
4	Vacuum Bagging	-	-	-	-	600	Airtight seal for resin infusion
5	Inject Epoxy Resin using Resin Transfer Moulding (RTM)	RTM	-	-	-	60	Vacuum setting
6	Curing composite	Curing Oven	-	-	-	30	Constant temperature of 80°C
7	Cool the composite	-	-	-	-	720	
8	Join blade halves with epoxy adhesive	Assembly Table	-	-	-	180	Requires proper alignment and bonding
9	Surface treatment with water-based epoxy coating	Paint Booth	Spray Gun	-	-	180	Needs to dry for 720 mins
10	Quality Inspection	-	-	-	-	30	Meet quality standards

Table 82: Operations list for the low-speed shaft

Part Name: Low-Speed Shaft		List Number: 2/10					
Date: 12/04/2024		Drawing Number: 2					
Quantity: 1		Planner: Sundus					
Op No	Description	Machine Tool	Tool	Cutting Speed (m/min)	Feed Rate (mm/rev)	Set Up & Op. Time (min)	Notes
1	Heat stainless steel at 1000 °C	Furnace	-	-	-	15	
2	Closed die forging of mould	Hydraulic Press	-	-	-	240	Length of 10 m
3	Rough turning of shaft Ø1.2m	CNC Vertical Lathe	Carbide tool	150	0.2	60	Remove excess material
4	Chamfer edges	CNC Lathe	Chamfering tool	100	0.1	30	Break sharp edges
5	Surface finishing	CNC Lathe	Carbide tool	50	0.05	200	Achieve desired surface finish
6	Drill 30 Ø80 mm holes	CNC Drilling	Twist Drill	30	0.1	90	
7	Quality Inspection & Deburr	-	Deburring Tool	-	-	60	Meet quality standards

Table 83: Operations list for the turbine hub

Part Name: Turbine Hub		List Number: 3/10					
Date: 12/04/2024		Drawing Number: 3					
Quantity: 1		Planner: Sundus					
Op No	Description	Machine Tool	Tool	Cutting Speed (m/min)	Feed Rate (mm/rev)	Set Up & Op. Time (min)	Notes
1	Heat the stainless steel at 1000 °C	Furnace	-	-	-	15	

2	Open die forging of mould	Forging Press	Hammer	-	-	180	
3	Drill 30 Ø80 mm diameter holes for mounting to blade	CNC Drilling	Twist drill	30	0.1	60	Need precise hole depth and alignment
4	Bore holes	CNC Boring	Boring Bar	30	0.05	90	Achieve precise bore diameter
5	Tap holes for bolt attachment	CNC Tapping Machine	Tap	20	0.03	120	Ensure correct thread alignment
6	Surface finishing	CNC Lathe	Carbide tool	50	0.05	120	surface finish of
7	Surface treatment with water-based epoxy coating	Paint Booth	Spray Gun	-	-	180	Needs to dry for 600 mins
8	Quality Inspection	-	-	-	-	60	Meet quality standards

Table 84: Operations list for the turbine nose cone

Part Name: Turbine Nose Cone		List Number: 4/10					
Date: 12/04/2024		Drawing Number: 4					
		Quantity: 1					
		Planner: Sundus					
Op No	Description	Machine Tool	Tool	Cutting Speed (m/min)	Feed Rate (mm/rev)	Set Up & Op. Time (min)	Notes
1	Milling of stainless steel surface	CNC Vertical Milling	Carbide end mill	50	0.2	120	Remove excess material
2	Cut E-fibre glass reinforcement	Waterjet Cutter	Waterjet Nozzle	12	-	5	
3	Place E-fibre glass into mould	Layup Table	-	-	-	15	
4	Vacuum Bagging	-	-	-	-	600	Airtight seal
5	Epoxy Resin mixing and infusion	RTM	-	-	-	60	Vacuum setting
6	Curing Composite	Curing Oven	-	-	-	30	Constant temperature of 80°C

7	Cooling the composite	-	-	-	-	720	
8	Surface treatment with water-based epoxy coating	Paint Booth	Spray Gun	-	-	180	Needs to dry for 720 mins
9	Quality Inspection	-	-	-	-	30	Meet quality standards

Table 85: Operations list for the M80 Barrel nuts

Part Name: M80 Barrel Nuts		List Number: 5/10					
Date: 12/04/2024		Drawing Number: 5					
		Quantity: 90					
		Planner: Sundus					
Op No	Description	Machine Tool	Tool	Cutting Speed (m/min)	Feed Rate (mm/rev)	Set Up & Op. Time (min)	Notes
1	Cold closed die forging of mould	Forging Press	Hammer	-	-	120	
2	Centre drill inner diameter	CNC Lathe	Centre Drill	50	0.1	20	
3	Rough turning of outer diameter Ø80 m	CNC Turning	Carbide bit	150	0.1	10	Remove excess material
4	Bore inner diameter	CNC Boring	Boring Bar	30	0.05	30	Achieve precise diameter
5	Cut internal threads	CNC Thread Mill	Thread Milling Cutter	20	0.05	45	
6	Chamfer edges	CNC Lathe	Chamfering tool	100	0.1	15	Break sharp edges
7	Quality Inspection & Deburr	-	Deburring tool	-	-	30	Meet quality standards

Table 86: Operations list for the M80 x 400 mm & M80 x 110 mm bolts

Part Name: M80 x 400 mm & M80 x 110 mm Bolts		List Number: 6/10					
Date: 12/04/2024		Drawing Number: 6					
		Quantity: 180 (400 mm) & 90 (110 mm)					
		Planner: Sundus					
Op No	Description	Machine Tool	Tool	Cutting Speed (m/min)	Feed Rate (mm/rev)	Set Up & Op. Time (min)	Notes
1	Cold closed die forging of mould	Forging Press	Hammer	-	-	120	
2	Centre drill inner diameter	CNC Lathe	Centre Drill	50	0.1	30	
3	Rough turning of outer diameter Ø80 m	CNC Turning	Carbide bit	150	0.2	15	Remove excess material
4	Cut external threads of	CNC Turning	Threading Tool	20	0.05	60	
5	Face off the bolt head and chamfer the edges	CNC Lathe	Carbide bit	100	0.2	30	Flat surface for bolt head
6	Quality Inspection & Deburr	-	Deburring tool	-	-	30	Meet quality standards

Table 87: Operations list for the Bearing House

Part Name: Bearing Housing		List Number: 7/10					
Date: 12/04/2024		Drawing Number: 7					
		Quantity: 3					
		Planner: Sundus					
Op No	Description	Machine Tool	Tool	Cutting Speed (m/min)	Feed Rate (mm/rev)	Set Up & Op. Time (min)	Notes
1	Heat the stainless steel at 1000 °C	Furnace	-	-	-	15	
2	Open die forging	Forging Press	Hammer	-	-	180	
3	Drill holes for mounting bolts	CNC Drilling	Twist Drill Bit	30	0.1	45	

4	Bore and thread 30 Ø80mm holes	CNC Boring	Boring Bar	50	0.2	120	Precise for bearing assembly
5	Chamfer edges	CNC Lathe	Chamfering tool	100	0.1	30	Break sharp edges for safety
6	Surface finishing	Grinding Wheel	-	20	0.05	60	Achieve desired surface finish
7	Quality Inspection & Deburr	-	Deburring tool	-	-	30	Meet quality standards

Table 88: Operations list for the pitch drive ring gear

Part Name: Ring Gear		List Number: 8/10					
Date: 12/04/2024		Drawing Number: 8					
		Quantity: 3					
		Planner: Sundus					
Op No	Description	Machine Tool	Tool	Cutting Speed (m/min)	Feed Rate (mm/rev)	Setup & Op. Time (min)	Notes
1	Heat the carbon steel at 1200 °C	Furnace	-	-	-	15	
2	Closed die forging	Forging Press	Hammer	-	-	180	
3	Rough milling of outer diameter	CNC Milling	End mill	100	0.3	90	
4	Drill centre	CNC Lathe	Centre Drill	50	0.1	120	
5	Bore the inner diameter	CNC Boring	Boring Bar	30	0.05	180	
6	Cut 288 internal gear teeth	CNC Hobbing	Gear Hob	40	0.1	180	
7	Chamfer edges	CNC Lathe	Chamfering tool	100	0.1	30	Break sharp edges for safety
8	Surface finishing	Shot Peening Machine	Shot Peening Nozzle	-	-	60	Achieve desired surface finish
9	Quality Inspection & Deburr	-	Deburring tool	-	-	30	Meet quality standards

Table 89: Operations list for the pitch drive pinion gear

Part Name: Pinion Gear		List Number: 9/10					
		Drawing Number: 9					
Date: 12/04/2024		Quantity: 3					
		Planner: Sundus					
Op No	Description	Machine Tool	Tool	Cutting Speed (m/min)	Feed Rate (mm/rev)	Setup & Op. Time (min)	Notes
1	Heat the low alloy steel at 850 °C	Furnace	-	-	-	15	
2	Closed die forging	Forging Press	Hammer	-	-	180	
3	Rough milling of outer diameter	CNC Milling	End mill	100	0.3	120	Remove excess material
4	Drill Centre	CNC Lathe	Centre Drill	50	0.1	120	
5	Bore the inner diameter	CNC Boring	Boring Bar	30	0.05	180	
6	Cut internal spline	CNC Machining	Broaching Tool	30	0.05	240	
7	Cut 27 external gear teeth	CNC Hobbing	Gear Hob	40	0.1	180	
8	Chamfer edges	CNC Lathe	Chamfering tool	100	0.1	30	Break sharp edges
9	Surface finishing	Shot Peening Machine	Shot Peening Nozzle	-	-	60	Achieve desired surface finish
10	Quality Inspection & Deburr	-	Deburring tool	-	-	30	Meet quality standards

Table 90: Operations list for the pinion coupling

Part Name: Pinion Coupling		List Number: 10/10					
Date: 12/04/2024		Drawing Number: 10					
		Quantity: 1					
		Planner: Sundus					
Op No	Description	Machine Tool	Tool	Cutting Speed (m/min)	Feed Rate (mm/rev)	Set Up & Op. Time (min)	Notes
1	Heat the carbon steel at 1200°C	Furnace	-	-	-	15	
2	Closed die forging	Forging Press	Hammer	-	-	180	
2	Drill centre	CNC Lathe	Centre Drill	50	0.1	60	
3	Rough turning of outer diameter Ø80 mm	CNC Turning	Carbide bit	150	0.2	60	Remove excess material
4	Bore the inner diameter	CNC Boring	Boring Bar	30	0.05	90	
5	Mill the external spline	CNC Milling	End mill	30	0.05	180	
6	Cut keyway	CNC Machining	Broaching Tool	30	0.05	90	
7	Chamfer edges	CNC Lathe	Chamfering tool	100	0.1	30	Break sharp edges for safety
8	Surface finishing outer diameter	CNC Lathe	Carbide tool	50	0.05	60	Achieve desired surface finish
9	Quality Inspection & Deburr	-	Deburring tool	-	-	30	Meet quality standards